

INVESTIGATION OF CREEP BUCKLING OF COLUMNS AND PLATES

PART III: CREEP BUCKLING EXPERIMENTS WITH COLUMNS OF 2024-0 ALUMINUM ALLOY

*RALPH PAPIRNO
GEORGE GERARD*

NEW YORK UNIVERSITY

JUNE 1961

**DIRECTORATE OF MATERIALS AND PROCESSES
CONTRACT No. AF 33(616)-5807
PROJECT No. 7381**

**AERONAUTICAL SYSTEMS DIVISION
AIR FORCE SYSTEMS COMMAND
UNITED STATES AIR FORCE
WRIGHT-PATTERSON AIR FORCE BASE, OHIO**

FOREWORD

This report was prepared by New York University under USAF Contract No. AF 33-(616)-5807. The contract was initiated under Project No. 7381, "Materials Application," Task No. 73812, "Data Collection and Correlation." The work was administered under the direction of the Materials Central, Directorate of Advanced Systems Technology, Wright Air Development Division, with Lt. William H. Hill and Dr. Ibrahim Ebcioğlu acting as project engineers.

This report covers work conducted from April 1960 through December 1960.

The authors wish to acknowledge the assistance of Mr. Martin Eisenberg of the Solid Mechanics Laboratory in the experimental program.

ABSTRACT

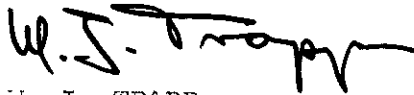
Experimental data for short time buckling and creep buckling of aluminum alloy 2024-O columns at 500°F were collected. Two slenderness ratios $L'/\rho = 40$ and $L'/\rho = 60$ were tested each with both simulated pinned ends and simulated fixed ends. In addition compressive short time and compressive creep data for the aluminum alloy material were collected.

A technique, whereby end shortening and central deflection data are autographically recorded both during the period when the creep load was being applied and during creep, was used. It was therefore possible to determine initial imperfections by the Southwell method for the creep buckling experiments. Data presented include initial imperfections as well as central deflection and end shortening data. Experimental relationships between applied stress and failure time are presented as well as an analysis of the central deflection and the end shortening data.

PUBLICATION REVIEW

This report has been reviewed and is approved.

FOR THE COMMANDER:



W. J. TRAPP
Chief, Strength and Dynamics Branch
Metals and Ceramics Laboratory
Directorate of Materials and Processes

TABLE OF CONTENTS

	Page
I INTRODUCTION	1
II MATERIALS TEST PROGRAM	2
1. Criteria of Material Selection	2
2. Material Evaluation Program	2
3. Short Time Compression Stress Strain Tests	3
4. Compression Creep Tests	4
5. Discussion of Material Properties Test Results	4
III COLUMN BUCKLING APPARATUS AND PROCEDURE	5
1. End Fixity Coefficient Tests	5
2. Column Creep Buckling Specimens	6
3. Experimental Accuracy	7
IV COLUMN BUCKLING TEST RESULTS	8
1. Short Time Buckling Data	8
2. Discussion of Short Time Buckling Data	9
3. Creep Buckling Failure Time Data	10
4. Discussion of Failure Time Results	12
5. End Shortening and Central Deflection Results	13
6. Discussion of End Shortening and Central Deflection Results	13
7. Bending Component of End Shortening	15
V CONCLUDING REMARKS	17
1. Experimental Techniques	17
2. Materials	17
3. Experimental Results for Columns	17
IV BIBLIOGRAPHY	19

LIST OF TABLES

Table		Page
1	Specimen Dimensions and Test Results for End Fixity Coefficient Tests of Aluminum Alloy 7075-T6 Flat End Columns, $L = 3.610$ in.....	6
2	Specimen Dimensions and Test Results for End Fixity Coefficient Tests of Aluminum Alloy 7075-T6 Roller End Columns, $L = 3.610$ in.....	6
3	Column Geometric Lengths for Various Configurations	7
4	Short Time Failure Data for Aluminum Alloy 2024-0 Columns at 500°F	9
5	Creep Buckling Failure Time Data, $L'/\rho = 40$ Columns. Relative Initial Imperfections Less Than .005	11
6	Creep Buckling Failure Time Data, $L'/\rho = 60$ Columns. Relative Initial Imperfections Less Than .005	12

LIST OF ILLUSTRATIONS

Figure		Page
1	Comparison of Short Time Stress-Strain Properties in Compression at 500°F Between 2024-0 and 5052-0 Aluminum Alloy	20
2	Preliminary Compression Creep Curves of 2024-0 Aluminum Alloy at 500°F and 8500 psi Applied Stress Used for Material Evaluation	20
3	Average Short Time Compression Stress-Strain Curves for 2024-0 Aluminum Alloy at 500°F	21
4	Average Compression Creep Curves for 2024-0 Aluminum Alloy at 500°F. Heat 3	22
5	Average Compression Creep Curves for 2024-0 Aluminum Alloy at 500°F. Heat 4	23
6	Roller Bearing End Restraints Simulating Simple Support	24
7	Flat End Restraints Simulating Fixed Ends	24
8	Column Specimen Installed in Roller Bearing End Restraints with End Shortening and Central Deflection Instrumentation Attached	24
9	Test Records for Short Time Buckling Test of 2024-0 Aluminum Alloy Column, $L'/\rho = 40$ with Roller End Restraints at 500°F	25
10	Test Records for Creep Buckling Test of 2024-0 Aluminum Alloy Column, $L'/\rho = 40$ with Roller End Restraints at 6320 psi and 500°F	25
11	Short Time Buckling Results for Anneal Heat 3 Experiment and Theory	26
12	Short Time Buckling Results for Anneal Heats 4 and 5 Experiment and Theory	26
13	Creep Buckling Results for Columns of $L'/\rho = 40$ Anneal Heat 3	27
14	Creep Buckling Results for Columns of $L'/\rho = 40$ Anneal Heats 4 and 5	27
15	Creep Buckling Results for Columns of $L'/\rho = 60$ Anneal Heat 3	28
16	Creep Buckling Results for Columns of $L'/\rho = 60$ Anneal Heats 4 and 5	28

LIST OF ILLUSTRATIONS

(Continued)

Figure		Page
17	Normalized Creep Buckling Results for All L'/ρ , All C Values, All Heats	29
18	End Shortening-Time, $L'/\rho = 40$, $\sigma_a = 5480$ psi	30
19	Central Deflection-Time, $L'/\rho = 40$, $\sigma_a = 5480$ psi	30
20	End Shortening-Time, $L'/\rho = 40$, $\sigma_a = 6320$ psi	30
21	Central Deflection-Time, $L'/\rho = 40$, $\sigma_a = 6320$ psi	31
22	End Shortening-Time, $L'/\rho = 40$, $\sigma_a = 6744$ psi	31
23	Central Deflection-Time, $L'/\rho = 40$, $\sigma_a = 6744$ psi	31
24	End Shortening-Time, $L'/\rho = 40$, $\sigma_a = 7165$ psi	32
25	Central Deflection-Time, $L'/\rho = 40$, $\sigma_a = 7165$ psi	32
26	End Shortening-Time, $L'/\rho = 60$, $\sigma_a = 5480$ psi	32
27	Central Deflection-Time, $L'/\rho = 60$, $\sigma_a = 5480$ psi	32
28	End Shortening-Time, $L'/\rho = 60$, $\sigma_a = 5600$ psi	33
29	Central Deflection-Time, $L'/\rho = 60$, $\sigma_a = 5600$ psi	33
30	End Shortening-Time, $L'/\rho = 60$, $\sigma_a = 6320$ psi	33
31	Central Deflection-Time, $L'/\rho = 60$, $\sigma_a = 6320$ psi	33
32	Relative Central Deflection at Failure in Creep Buckling	34
33	Diagram of Typical End Shortening Behavior	34
34	Deflected Column Geometry	35
35	Theoretical Bending Component of End Shortening Compared with Test Data for All Creep Buckling Experiments	36
36	Theoretical Bending Component of End Shortening Compared with Test Data from Four Experiments with Different Initial End Shortening Components	37

Contrails

I INTRODUCTION

In a previous investigation (1,2), the creep buckling of Ti-7Al-4Mo titanium alloy columns was studied. The alloy chosen was one which was potentially useful in aerospace vehicles. However high creep resistance, sharp knee of the stress strain curve in the yield region and scatter of properties of the titanium alloy material limited our experiments to columns where $L'/\rho = 40$ at 950°F and loaded to within 6% of the short time buckling load for creep buckling within reasonable times.

In the current investigation columns of aluminum alloy 2024-0 were tested. This material was selected primarily with the view of comparing experiments with theory. Columns of two slenderness ratios, $L'/\rho = 40$ and $L'/\rho = 60$, with two end fixity conditions, pinned and fixed, were tested over a wide range of applied stresses down to 60% of the short time strength. The two end fixity conditions bracketed the range of values of end fixity coefficient from one to approximately four in order that any differences in creep buckling behavior over this range might be discerned.

The various data collected for each of the experiments are given in this report in a form which may be useful to other workers in the field. In addition, a separate report is now being prepared which gives the results of a theoretical investigation and includes a comparison of theory with the pertinent test data.

Criteria had been established for the choice of a material for creep buckling experiments to result in reasonably short creep buckling times. It appeared that two aluminum alloys 5052-0 and 2024-0 would most closely fit the criteria. A short test program, herein described, established that the 2024-0 alloy more closely satisfied the criteria and it was chosen as the test material for the investigation. Compressive short time and creep properties were determined for the material.

Both short time buckling tests, and creep buckling tests at a variety of applied stresses, were performed. End shortening and central deflection were measured during a majority of both types of experiments and the collected data are given herein. It has been found that the end shortening measurements, heretofore generally neglected in other similar investigations, are significant for relating the creep buckling behavior of the column to the creep properties of the material from which the column has been fabricated.

Three separate areas of investigation have been considered:

1. Critical times for columns over a large range of applied stresses.
2. Relation between critical times for fixed end columns with those for pin end columns for the same range of applied stresses.
3. Relations between end shortening, central deflection and critical time.

The test procedures and results for each of the areas are given in detail in this report.

Manuscript released by the authors on January 31, 1961 for publication as a WADC Technical Report.

WADC TR 59-416 Pt III

Contrails

II MATERIALS TEST PROGRAM

1. Criteria of Material Selection

The philosophy adopted in planning the current creep buckling experiments was to perform the greatest number of experiments under a large variety of different conditions within the time allotted for the investigations. Such a philosophy naturally led to a set of criteria for choosing a material from which the column specimens would be fabricated since:

1. Scatter: The material should have small scatter of properties making unnecessary statistically large numbers of experiments at each condition of loading, slenderness ratio and end fixity value.
2. Creep Rates: The material should have appreciable creep rates in order that each individual experiment, especially those at the lower stress levels, could be completed in a matter of hours. This would assure that many specimens could be tested within the contract time.
3. Stress Strain Curve: The material should have a rounded knee of the stress-strain curve in the yield region which in addition to No. 2 above would allow a large range of applied stresses in the column experiments and would assure that each experiment would terminate within a reasonable time.
4. Machinability: As a matter of efficiency in specimen preparation, the material should be machinable so that large numbers of specimens could be prepared in as short a time as possible.
5. Changes During Test: The material should not age or otherwise change in properties during the anticipated test times up to ten hours.

2. Material Evaluation Program

Both the 2024-0 and the 5052-0 aluminum alloys were suggested as materials which would most likely meet many of the criteria above. These were evaluated by means of compression short time and compression creep tests at 500°F.

Solid cylindrical specimens nominally 3/8 inch in diameter and 2 inches long were fabricated from blanks cut from 3/8 inch thick plates of aluminum alloys 2024-T4 and 5052-H34. The latter was supplied through the courtesy of Dr. M. Holt of the Aluminum Company of America. It was possible to limit the maximum variation in diameter from the mean value in individual specimens to ± 0.0001 inches in both alloys although considerably greater effort was required for the 5052 alloy than for the 2024 alloy. After finishing operations were completed, all specimens were

annealed to the "0" condition. The procedures recommended by Alcoa for each of the alloys were as follows:

2024: 775°F, 2 hours; cool at a maximum rate of 50°F/hr to 500°F, air cool.
5052: Heat to 650°F, furnace cool.

By using annealed material we anticipated that criterion No. 5 would be met by both alloys.

Short time compression stress-strain tests at 500°F were performed in a pneumatic testing machine using a differential capacitor extensometer over a one inch gage length. The test procedures we employed were the same as those used previously (2). For each alloy these tests were performed at an average strain rate of approximately 0.05 min^{-1} , a value we anticipated using in the creep buckling experiments. The test results are given in Figure 1.

Several features are evident in comparing the results for the two alloys:

1. The 2024-0 alloy shows much less scatter of properties.
2. The 2024-0 alloy has a rounder knee of the stress strain curve in the yield region.

On the basis of these observations the 2024 alloy was superior to the 5052 alloy using criteria Nos. 1 and 3 and its machining qualities made it superior on the basis of criterion No. 4.

Before the 2024-0 alloy was accepted, three creep tests were performed at 500°F and 8500 psi stress to check both the scatter and the attainable creep rates. The procedures used in creep testing involved the same pneumatic testing machine, extensometer and autographic recording equipment previously described (1,2). The results of the three separate tests, shown in Figure 2, met criteria 1 and 2 and led to the acceptance of aluminum alloy 2024-0 as the test material.

In the test program all specimens were machined from the 2024 alloy in the more easily handled T-4 condition, including all finishing operations. The finished specimens were wrapped in aluminum foil and annealed in a number of separate heats. This procedure of machining in the T-4 condition avoided possible work hardening of the material which might occur during machining of the annealed specimens. Included in each heat were both compression specimens and column buckling specimens.

There were differences in mechanical properties in the various heats, with these differences being more marked in the compression creep data than in the compression stress-strain data. Consequently the specimens, both column and material properties, have been identified according to heat number to insure that data comparisons will be made on the basis of material all from the same heat.

3. Short Time Compression Stress-Strain Tests

Column creep buckling studies were conducted with specimens from three specific annealing heats, 3, 4, and 5. Although some preliminary experiments were conducted with other batches, these are not reported in the finally collected data. Shown in Figure 3 are average compressive stress strain curves for the two heats

of interest. Heat 5 is generally similar to heat 4.

The procedures used in collecting the data were identical with those employed in the material evaluation program. Great care was exercised in the manufacture of the specimens to limit diameter variations to ± 0.0001 inch and to maintain parallelism of the ends within approximately 1 minute of arc.

4. Compression Creep Tests

Compression creep tests were performed at 500°F using autographic procedures already described (1,2) at a number of stress levels pertinent to the creep buckling experiments. Data for heat No. 3 are given in Figure 4 and that for heat No. 4 are given in Figure 5. These data, although assembled here, were collected at various times during the creep buckling program.

5. Discussion of Material Properties Test Results

The short time and creep properties of heat No. 3 are generally lower than those of heat No. 4. A careful check of our procedures indicated that the differences were probably due to differences in the cooling rate from 775°F to 500°F during the anneal cycle. Although the differences between the two heats in the average stress strain curves are relatively small (less for example than the scatter in the 5052 alloy) these differences between heats are of greater magnitude in the creep properties and hence had to be taken into account in the analysis of the creep buckling data.

III COLUMN BUCKLING APPARATUS AND PROCEDURES

In the experiments performed, four different configurations were tested: two slenderness ratios, $L'/\rho = 40$ and $L'/\rho = 60$, and two end conditions, roller ends and flat ends. For each condition of slenderness ratio and end fixity both short time and creep buckling experiments were performed.

The roller bearing end restraint mechanisms, previously employed in the titanium alloy creep buckling study were slightly modified by the removal of four of the end rollers which were not required for the lower load levels of the aluminum columns. A photograph of a specimen installed in the roller end restraints is shown in Figure 6. A new set of flat end supports, simulating fixed end boundary conditions, was constructed for the aluminum columns. These consist simply of hardened steel blocks with specimen positioning tabs and with a set of pins installed to facilitate end shortening measurements. These are shown in Figure 7.

The same procedures employed previously for conducting both the short time and creep buckling experiments were used for the aluminum columns. Central deflection and end shortening were measured and recorded autographically. A slight modification was made in some of the tests in our autographic recording procedure. Where previously a time base with a four hour sweep had been used, the time scale in a number of the current experiments was expanded by a factor of approximately thirty to obtain higher resolution. This was necessary since the overall times in our current experiments with aluminum columns were considerably shorter than those which were conducted previously with the Ti-7Al-4Mo titanium alloy columns. A photograph of a specimen installed in the roller bearing end restraints with end shortening and central deflection instrumentation attached is shown in Figure 8.

1. End Fixity Coefficient Tests

Short time tests with elastic columns were conducted with each of the end restraint configurations to determine the experimental value of the end fixity coefficient. It was to be expected that in the case of the fixed ends, especially, there would be some departure from the theoretical value $C = 4$.

Columns of aluminum alloy 7075-T6 were designed to buckle elastically at room temperature. Extreme care was exercised in the manufacture of these test columns to limit variations of width and thickness along each of the specimens to ± 0.0002 inches. The specimen dimensions and test results for simulated fixed end columns are given in Table 1 while those for the simply supported ends are given in Table 2. The values of the end fixity coefficient were computed from

$$C = L^2(\sigma_f)_0 / \pi^2 \rho^2 E \quad (1)$$

where

C	end fixity coefficient
L	geometric length of column, in.
$(\sigma_f)_0$	experimental short time strength, psi.
ρ	radius of gyration, in.
E	modulus of elasticity, psi.

In making the computation, the compression value of the modulus of elasticity $E = 10.6 \times 10^6$ psi for the 7075-T6 aluminum alloy was used. This value had been experimentally verified previously. Southwell analyses were performed on the data. The computed initial imperfections are given in terms of specimen thickness in Tables 1 and 2.

Table 1 - SPECIMEN DIMENSIONS AND TEST RESULTS FOR END FIXITY COEFFICIENT TESTS OF ALUMINUM ALLOY 7075-T6 FLAT END COLUMNS, $L = 3.610$ in.

Specimen	Width in.	Thickness in.	Radius of Gyration ρ , in.	Observed Strength, psi.	C	Relative Initial Imperf. (w_0/t)
75-1	.2201	.1104	.0318	31,000	3.80	.002
75-2	.2204	.1106	.0319	30,750	3.77	.006
75-4	.2197	.1098	.0316	30,000	3.72	.004
75-5	.2202	.1096	.0315	30,000	3.74	.008
75-6	.2204	.1096	.0315	30,000	3.74	.005

Average value $\bar{C} = 3.75$

Table 2 - SPECIMEN DIMENSIONS AND TEST RESULTS FOR END FIXITY COEFFICIENT TESTS OF ALUMINUM ALLOY 7075-T6 ROLLER END COLUMNS, $L = 3.610$ in.

Specimen	Columns Width in.	Thickness in.	Radius of Gyration ρ , in.	Observed Strength, psi.	C	Relative Initial Imperf. (w_0/t)
75-7	.2504	.1253	.0362	10,230	.98	less than .02
75-8	.2500	.1255	.0362	10,100	.96	.020
75-9	.2506	.1253	.0362	10,000	.95	.012

Average value $\bar{C} = .96$

The average value of the end fixity coefficient for the roller end restraints was deemed sufficiently close to the theoretical value, hence the value $C = 1$ was assumed for the experiments.

2. Column Creep Buckling Specimens

Rectangular cross section specimens of cross section dimensions nominally $1/8 \times 1/4$ inches were employed in all experiments. Two slenderness ratios $L'/\rho = 40$ and $L'/\rho = 60$ were used in the experiments. The quantity L' is defined as:

$$L' = L/C^{1/2} \quad (2)$$

where L' reduced length of column, in.

L geometric length of column, in.

C end fixity coefficient

The values of L for the various configurations are given in Table 3 below:

Table 3 - COLUMN GEOMETRIC LENGTHS FOR VARIOUS CONFIGURATIONS.

C	L'/ρ	L, in.
3.75	40	2.80
3.75	60	4.20
1.0	40	1.44
1.0	60	2.16

Actual specimen dimensions, obtained by micrometer caliper, were used to determine the slenderness ratio values. The variation in L'/ρ value among all the individual specimens from the desired value was less than 0.5 percent.

3. Experimental Accuracy

Much the same experimental environment existed in both the materials test program and the buckling program, hence the experimental accuracy for each are comparable. A detailed statement of the magnitude of error in our experimental set-up has already been given previously (1,2), however for convenience this statement is summarized below:

a) Extensometers for strain and end shortening:

Stability within 0.1% per day. Linear range for 1% linearity \pm 0.050 inch. Calibrated daily.

b) Loading system 0.5%.

c) Initial imperfections of specimens - maximum 2% of thickness, average 1% of thickness.

d) Temperature variation over 3 inch length \pm 1°F temporal variation \pm 2°F for the test periods.

e) Autographic recorders - calibrated daily - stability 0.25% per month.

f) Timing - Stop watch with least count .01 minutes. Autographic short time recorder - calibrated by stop watch.

IV COLUMN BUCKLING TEST RESULTS

The data for all experiments, both short time and creep buckling, are given herein in tables and charts. In the data the strength of the column for the short time experiments and the failure time of the column for the creep buckling experiments are recorded. In all experiments there was a slow increase of deflection of the center of the column and end shortening prior to collapse; however when collapse did occur, it was catastrophic and accompanied by an audible "ping." At failure both the end shortening and central deflection recorder arms moved suddenly off scale. The recorded point of failure was taken as that point when the end shortening recorder arm suddenly increased in velocity; this point was not difficult to ascertain since the ink trace became quite faint because of the high pen velocity. Shown in Figure 9 are typical recordings for a short time test and in Figure 10 typical recordings for a creep buckling test.

The central deflection-stress data, obtained during loading were analyzed by the Southwell method to obtain initial imperfections. These data are given in the tables in non-dimensional form as fractions of the thickness of the column. The values are generally quite small and reflect the precision of manufacture of the specimen and of the alignment of the specimen in the testing machine.

All the data were collected at a nominal temperature of $500^{\circ}\text{F} \pm 2^{\circ}\text{F}$ and hence temperatures are not recorded in the tabulation.

1. Short Time Buckling Data

The results of short time experiments are given in Table 4 below. It should be noted that the properties of anneal heat No. 3 are different from those of heats 4 and 5. The strength data are plotted in Figure 11 for heat 3 and Figure 12 for heats 4 and 5, together with the appropriate theoretical column curves for both the tangent modulus theory and the reduced modulus theory.

For the tangent modulus the relation

$$\sigma_{cr} = \pi^2 E_t / (L'/\rho)^2 \quad (3)$$

was used, while for the reduced modulus

$$\sigma_{cr} = \pi^2 E_r / (L'/\rho)^2 \quad (4)$$

was used. The reduced modulus was computed from

$$E_r = 4EE_t / (E^{1/2} + E_t^{1/2})^2 \quad (5)$$

Where

σ_{cr} short time buckling stress, psi.

E modulus of elasticity, psi.

E_t tangent modulus, psi.

E_r reduced modulus, psi.

The values of E and E_t were found from the appropriate short time stress-strain curves given in Figure 3.

Table 4 - SHORT TIME FAILURE DATA FOR ALUMINUM ALLOY 2024-0 COLUMNS AT 500°F.

Specimen No.	Anneal Heat No.	Slenderness Ratio (L'/ρ)	End Fixity Coefficient, C	Observed Strength, psi.	Relative Initial Imperf. (w_o/t)
C 9-4	3	40	3.75	9500	0.01
D 13-5	3	40	3.75	9750	0.01
D 12-2	3	40	3.75	10000	0.01
D 4-4	3	40	3.75	10300	+
C 11-3	3	40	3.75	9900	+
D 5-7	3	60	3.75	8100	+
D 9-4	3	60	3.75	8450	+
D 10-5	3	60	3.75	8700	+
D 27	5	40	1	8750	.045
D 96	5	40	1	9250	.032
D 11-2	4	40	1	8950	.01
D 502	4	40	3.75	10650	.01
C 6-1	4	40	3.75	10800	.01
D 91	5	60	1	8050	.013
D 56	5	60	1	7800	.032
C 4-1B	5	60	1	8800	.01
D 15-5	4	60	3.75	8025	.013
D 16-2	4	60	3.75	8150	.026
D 3-2	4	60	3.75	8900	.01
C 15-1A	4	60	1	8150	+

+ No central deflection instrumentation employed.

2. Discussion of Short Time Buckling Data

A number of features are apparent from Figures 11 and 12. The data are all generally higher than the theoretical tangent modulus relation Eq.(3) predicts. The data for the roller end columns shown in Figure 12 however fall between the predictions of Eq.(3) and those of the reduced modulus Eq.(4). The agreement here with theory is considered satisfactory with Eq.(3) and Eq.(4) defining upper and lower bounds to short time plastic buckling. In both Figures 11 and 12 however the data for fixed end columns are higher than the predictions of the reduced modulus, Eq.(4).

In an attempt to determine whether the lateral deflection instrumentation was causing a restraint, a number of tests were performed in which no lateral deflection instrumentation was used. These tests are identified in Table 4. For $L'/\rho = 40$, the observed failure strengths vary by only 3%. Hence it could be concluded that if the instrumentation was exercising a restraint, the effect on the failure stress was smaller than the effect of the scatter of the data. The reasons for the high values for the fixed end columns have not been explained.

3. Creep Buckling Failure Time Data

Failure times and other pertinent data are given in Table 5 for $L'/\rho = 40$ and Table 6 for $L'/\rho = 60$. Included in the tables are the ratios of the applied stress, σ_a to the average short time strength, $(\sigma_f)_0$, for the appropriate heat number and column configuration. Initial imperfection data were derived from Southwell analyses of the central deflection measured during the application of the creep load. In all cases the initial imperfections were less than 0.5% of the thickness, hence these negligibly small values are not recorded in the tables. The failure time data are also shown graphically in Figures 13 and 14 for $L'/\rho = 40$ and Figures 15 and 16 for $L'/\rho = 60$. Since there was a variation in properties among different anneal heats of the material, it has been convenient to normalize the applied stress data to the short time values in the manner previously indicated in order to make comparisons between data of the various heats. The normalization procedure allowed plotting all the collected creep buckling data from all heats on the same chart, shown in Figure 17. The curves shown in Figures 13-17 are empirical and were drawn to represent a best fit for the experimental data.

Table 5 - CREEP BUCKLING FAILURE TIME DATA $L'/\rho = 40$ COLUMNS. RELATIVE INITIAL IMPERFECTIONS LESS THAN .005.

Specimen No.	Anneal Heat	End Fixity Coefficient, C	Applied Stress, σ_a , psi.	Short Time Strength, $(\sigma_f)_o$, psi.	Applied Stress Ratio $\sigma_a/(\sigma_f)_o$	Failure Time, min.
D 55	3	3.75	9440	9950	.95	0.16
C 85	3	3.75	9000	9950	.91	.38
D 12-4	3	3.75	8950	9950	.90	.16
D 9-2	3	3.75	8450	9950	.85	.38
D 10-3	3	3.75	7950	9950	.80	.53
D 2-3	3	3.75	7950	9950	.80	1.24
D 18-5	4	3.75	7160	10,700	.67	8.50
D 15-3	4	3.75	7160	10,700	.67	10.25
D 14-2	4	3.75	6740	10,700	.63	49.56
C 17-2	4	3.75	6740	10,700	.63	33.16
C 13-5	4	3.75	6320	10,700	.59	30.40
C 14-5	4	3.75	6320	10,700	.59	19.42
C 11-7	5	1	7160	8950	.80	.85
C 3-1	5	1	7160	8950	.80	1.10
D 11-1A	4	1	7160	8950	.80	.70
D 4-1	5	1	6320	8950	.70	3.92
C 2-2	5	1	6320	8950	.70	12.76
C 4-1A	4	1	6320	8950	.71	3.3
C 14-1	5	1	5480	8950	.61	33.71
C 10-2A	4	1	5480	8950	.61	21.69

Table 6 - CREEP BUCKLING FAILURE TIME DATA FOR $L'/\rho = 60$ COLUMNS. RELATIVE INITIAL IMPERFECTIONS LESS THAN .005.

Specimen No.	Anneal Heat	End Fixity Coefficient, C	Applied Stress σ_a , psi.	Short Time Strength $(\sigma_f)_o$, psi.	Applied Stress Ratio $\sigma_a/(\sigma_f)_o$	Failure Time, min.
C 2-7	3	3.75	8000	8450	.95	.22
D 13-7	3	3.75	8000	8450	.95	.14
C 3-6	3	3.75	7590	8450	.90	.20
C 6-4	3	3.75	7590	8450	.90	.15
C 9-6	3	3.75	7160	8450	.85	.42
C 8-7	3	3.75	7160	8450	.85	.31
C 11-5	3	3.75	6740	8450	.80	1.90
C 12-4	3	3.75	6740	8450	.80	.72
D 17-6	4	3.75	6320	8350	.76	2.24
D 18-7	4	3.75	6320	8350	.76	2.90
C 14-6	4	3.75	5600	8350	.67	3.75
C 13-7	4	3.75	5600	8350	.67	5.50
C 16-5	4	3.75	5480	8350	.66	18.97
C 17-4	4	3.75	5480	8350	.66	6.55
C 9-3	5	1	6320	7900	.80	.78
D 11-2B	4	1	6320	8400	.75	1.88
D 14-1	5	1	5480	7900	.69	2.50
C 15-2A	4	1	5480	8400	.65	3.88

4. Discussion of Failure Time Results

It was evident from the short time buckling tests that there were differences in behavior between the roller end columns and flat end columns especially for $L'/\rho = 40$. These differences are also manifested in the creep buckling results as shown in Figures 14 and 16 where the roller end columns are shown to fail in shorter times than those with flat ends. This behavior is consistent with the short time failure behavior, although no ready explanation for the phenomenon suggests itself.

The material in anneal heat 3 has lower short time stress-strain properties than those of heats 4 and 5 and the former exhibits higher creep rates as well. These differences are reflected in both the short time and creep buckling behavior of the columns. Short time strengths are lower and failure times are shorter for columns of heat 3.

In an attempt to make a rational comparison of the behavior of all columns, stresses were normalized to the short time failure stress. For each end fixity condition, slenderness ratio and material, the applied stress for creep buckling was

computed as a certain percentage of the short time buckling stress for the same condition and the results were plotted in the form shown in Figure 17. The essential similarity of behavior of all columns is evident in these normalized results. The scatter band is relatively small, being $\pm 5\%$ in the stress at the short time value. One virtue of the representation shown in Figure 17 is that major differences in material properties among heats are suppressed and that the scatter which is present in the figure is a reflection only of the natural scatter of material properties in any one heat and small uncontrollable differences in the individual experiments.

The consistency of the results shown in Figure 17, when compared with the results represented in conventional form in Figures 13-16 indicate the definite relationship between short time buckling and creep buckling behavior. Small differences in the short time strength of columns with different end fixity or of a different heat are manifested by larger differences in failure times and it is only when the stresses are normalized that these differences disappear.

5. End Shortening and Central Deflection Results

The end shortening data were collected in non-dimensionalized form as an end shortening strain with the column length used as the gage length. Since end shortening data were determined from the changing separation distance of the heads of the testing machine they not only reflect the creep strain of the columns but also the effects of column lateral deflections, the probable non-uniform strain distribution at the column ends, and initial slop in the system.

Central deflections were measured from a line of reference, which for all values of central deflection, joined the center of the end faces of the columns.

Results are given in Figures 18-31. Each figure gives either end shortening time or central deflection-time data for a particular value of applied stress for columns with the longer creep buckling times. Included with the end shortening data in each figure is the creep curve for the appropriate applied stress.

6. Discussion of End Shortening and Central Deflection Results

Internal consistency of behavior in experiments is evident by a comparison of the end shortening and central deflection results for individual experiments. In most of the experiments at any particular stress level, those columns which buckled in the shortest time showed the greatest initial central deflection and the greatest departure of end shortening from the appropriate creep curve.

In the experiments, the central deflection at failure is difficult to ascertain exactly. The maximum central deflection which could be recorded in the majority of the experiments was of the order of .050 inch or 40% of the thickness of the column. This value was generally realized some 2-4 seconds before failure of the column. However the slope of the deflection-time curve generally increased very rapidly prior to the .050 inch displacement. The raw deflection data were analyzed and charted as shown in Figures 19, 21, etc. The failure value of the central deflection was taken from the analyzed data as the value where the slope of the curve became vertical. This involved a rather arbitrary choice and hence such values, shown in Figure 32, are only a rough estimate of the actual central deflection-behavior at column failure.

The trend in Figure 32 however is quite clear. With failure times below 5 minutes, the central deflection value is only 15% of the thickness of the column. For the longer failure times the central deflection goes to larger values though generally remaining less than 40% of the thickness.

Typical end shortening behavior has been illustrated in the diagram in Figure 33.

During the period of load application to the column at the beginning of a test, the measured end shortening is larger than the strain measured during load application in a compressive creep test. The magnitude of this difference will be governed by the initial conditions of the test and includes the following effects:

- a) Small deflections in the steel end plates of the loading rams of the testing machine.
- b) Non uniform strain at the column ends.
- c) Small geometric imperfections in the columns.
- d) Initial slop in the system.

An estimate of the magnitude of the difference can be obtained by displacing the creep curve upwards to the end shortening curve to achieve a good fit in the initial knee region. This displacement is shown in Figure 33 and the quantity Δe_i is a measure of the difference between the two curves.

After the creep load has been applied it can be observed that the end shortening rate is higher than the creep rate. In all probability bending in the column as evidenced its central deflection and higher creep rates at the ends of the column contribute further to the departure from the creep curve. The latter may be a consequence of stress concentrations at the plane of contact between the column ends and the steel end plates. This latter effect is not included in the creep curve since the creep extensometers are attached directly to the compressive creep specimens away from the ends.

It is possible, as subsequently will be shown, to compute the bending component of end shortening from the central deflection values. This component is shown in Figure 33 as e_b . The component of end shortening due to end effect is also shown and is designated as Δe_f .

In summary, the end shortening measured at column failure consists of the following four components:

1. A creep component, ϵ_f .
2. A bending component, e_b .
3. An initial effect Δe_i .
4. A column end creep effect Δe_f .

Items 1 and 2 can be considered characteristic of the creep buckling phenomena while items 3 and 4 are introduced by the test conditions and are extraneous. The true end shortening at failure is given by

$$e_{net} = \epsilon_f + e_b \quad (6)$$

The quantity ϵ_f may be obtained from the pertinent compressive creep data while e_b must be derived from the central deflection data.

7. Bending Component of End Shortening

The column in the straight and the deflected positions is shown schematically in Figure 34. With a column of initial length L_o , when compressed and then deflected, the straight line distance between the column ends is L . The end shortening is given by

$$e_b = \Delta L / L_o \quad (7)$$

However

$$\Delta L = L_o - L \quad (8)$$

Then

$$e_b = (L_o - L) / L_o \quad (9)$$

The length of the column in the deflected form is

$$S = L_o (1 - \epsilon_{\text{creep}}) \quad (10)$$

Since the creep strain is small with respect to unity

$$S = L_o \quad (11)$$

Combining Eq.(9) with Eq.(11)

$$e_b = (S - L) / L_o \quad (12)$$

It is now assumed that the shape of the deflected column can be approximated by a sine wave, as shown in Figure 34. The equation of the column can be given as

$$y = w \sin (\pi x) / L \quad (13)$$

where w is the deflection at the center of the column. The length of arc of any continuous plane curve is given by

$$S = \int_0^x [1 + (y')^2]^{1/2} dx \quad (14)$$

Performing the appropriate operations on Eq.(13) and setting the limits of integration between $x = 0$ and $x = L/2$

$$S = 2 \int_0^{L/2} [1 + (\pi w / L)^2 (1 - \sin^2 \pi x / L)]^{1/2} dx \quad (15)$$

Substituting $z = \pi x/L$, making the appropriate changes in the limits of integration, and making the assumption that the central deflection w is small in comparison with the column length Eq.(15) can be transformed to

$$S = (2L/\pi)(1+k^2)^{1/2} \int_0^{\pi/2} (1-k^2 \sin^2 z)^{1/2} dz \quad (16)$$

where

$$k = \pi(w/L) \quad (17)$$

Substituting Eq.(16) into the numerator of Eq.(12) with the added assumption that $L_0 = L$

$$e_b = (2/\pi)(1+k^2)^{1/2} \int_0^{\pi/2} (1-k^2 \sin^2 z)^{1/2} dz - 1 \quad (18)$$

It can be shown that Eq.(18) will also hold for columns where there is one full cycle sine wave with the appropriate changes in notation.

The integral given in the right hand side of Eq.(18) is an elliptic integral of the second kind, a function whose values have been tabulated and hence Eq.(18) can easily be evaluated. The magnitude of the end effects of the end shortening of columns may be found by comparing the magnitude of e_b as derived from Eq.(18) with the end shortening for comparable central deflection values after the initial component, Δe_i , and the compressive creep component, ϵ_{creep} , have been removed. This has been done in Figure 35. The magnitude of the difference between the experimental points and the theoretical expression indicates that this so called "end effect" can be relatively large. In Figure 36, the data for four different creep buckling experiments have been shown in logarithmic coordinates. In these experiments the initial component of end shortening varied from $0 \leq \Delta e_i \leq 1500$ microinch/inch. There is a slight trend discernible in which the larger values of initial effect are associated with the larger values of end effect and vice versa, but the data cannot be considered in any way conclusive. This effect illustrated in Figures 35 and 36 may add some uncertainty to experimental results when compared with theory.

Contrails

V CONCLUDING REMARKS

The experimental investigation has been summarized below in three separate categories: Experimental Techniques, Materials, and Experimental Results for Columns. The conclusions, although not specifically delineated as such are implicit in the summaries given below.

1. Experimental Techniques

It has been possible to simulate simple support boundary conditions for columns by the use of a roller bearing end restraint whose center of rotation is at the end of the column. Fixed end boundary conditions were simulated by the use of flat end columns resting on a rigid support. Tests using elastic columns indicated that end fixity coefficient values obtained were 1.0 for the roller ends and 3.75 for the flat ends, thus a range of end fixity conditions were tested in the program. Two slenderness ratios $L'/\rho = 40$ and $L'/\rho = 60$ were tested covering a range of column lengths.

During both short time buckling and creep buckling experiments a continuous record of both end shortening and central deflection was obtained autographically. The central deflection in all creep buckling experiments and the end shortening in many creep buckling experiments were autographically recorded as a function of stress during the initial loading. It was possible therefore to perform Southwell analyses on the central deflection data at 500°F for both the short time and the creep buckling experiments.

Using a technique developed in this investigation for compressive creep tests, the stress-strain behavior of the specimen during the application of the creep load at 500°F was recorded. Hence it was possible to obtain the complete loading history of the specimen. In this connection it should also be pointed out that it was also possible to control the strain rate during the application of the creep load to be comparable with the strain rate employed in applying the load to the columns in the creep buckling experiments.

2. Material

The material for this phase of the investigation, aluminum alloy 2024-0, was chosen on the basis of a set of criteria established for creep buckling experiments by means of a test program. For the most part, the criteria were met in all categories and consequently the 2024-0 alloy turned out to be a suitable material for the experiments. However, differences in properties, which may have resulted from small differences in the annealing procedure among various batches of specimen material, were observed. These differences were relatively small in the short time stress-strain properties at 500°F, but were significantly larger for compressive creep at the same temperatures. Because of the differences in properties among heats, it was necessary to collect separate data for each heat. When data for a particular heat were compared, the scatter in compressive creep properties was relative small.

3. Experimental Results for Columns

In short time buckling experiments, the strengths of simulated pin end columns were lower than those for fixed end columns, with the differences being greater for

the $L'/\rho = 40$ specimens. All short time buckling results were higher than those predicted by the tangent modulus theory. However, the results for the pin ended specimens fell between the predictions of the tangent modulus and the reduced modulus theories.

The creep buckling data are consistent with the short time data in that the simulated pin end columns fail in shorter times than simulated fixed end columns at the same stress level. It has been possible to make comparisons between the two end conditions and also between columns fabricated from materials of different properties by using a normalization procedure in which the applied stresses are normalized to the short time strength. It is significant to note when this normalization procedure is employed, failure times for both slenderness ratios, $L'/\rho = 40$ and $L'/\rho = 60$, may also be compared. It was possible in the normalized diagram in Figure 17 to show the experimental data for all experiments both short time and creep buckling, for all material properties, both boundary conditions and both slenderness ratios.

The applied stress-failure time experiments relation shown in Figure 17 extends over a wide range of applied stresses, $1 \geq \sigma_a/(\sigma_f)_0 \geq 0.6$, yet for even the lowest values of applied stress, the column fails within one hour. The use of a material with a rounded knee stress-strain curve, one of the criteria originally set for choice of material, has permitted this wide range of conditions, yet with failure occurring within a reasonable time. Hence a large number of creep buckling experiments have been possible during this investigation.

Although only rough estimates could be made of the value of central deflection at failure, there is a definite trend in the central deflection-failure time data. For those columns which failed in five minutes or less the failure central deflection value was below 15% of the column thickness. For columns which failed in ten minutes or more the central deflection was generally less than 40% of the thickness.

It has been shown that other effects besides those of creep and those resulting from the bending of the column make up the total end shortening of a column in a creep buckling experiment. Initial effects are manifested at the very beginning of a creep buckling experiment when central deflections due to bending are small and are probably the result of the experimental set up of the test. An end shortening analysis, using the central deflection data, reveals other contributions to the end shortening data which are extraneous to creep buckling. These are possibly due to non uniform straining at the column ends where the creep load is applied and probably result from stress concentrations.

VI BIBLIOGRAPHY

1. Papirno, R. and Gerard, G., "Investigation of Creep Buckling of Columns and Plates Part I: Elevated Temperature Properties of the Test Material Ti-7Al-4Mo Titanium Alloy," WADC Technical Report 59-416 Part I, November 1959.
2. Papirno, R. and Gerard, G., "Investigation of Creep Buckling of Columns and Plates Part II: Creep Buckling Experiments with Columns of Ti-7Al-4Mo Titanium Alloy," WADC Technical Report 59-416 Part II, July 1960.

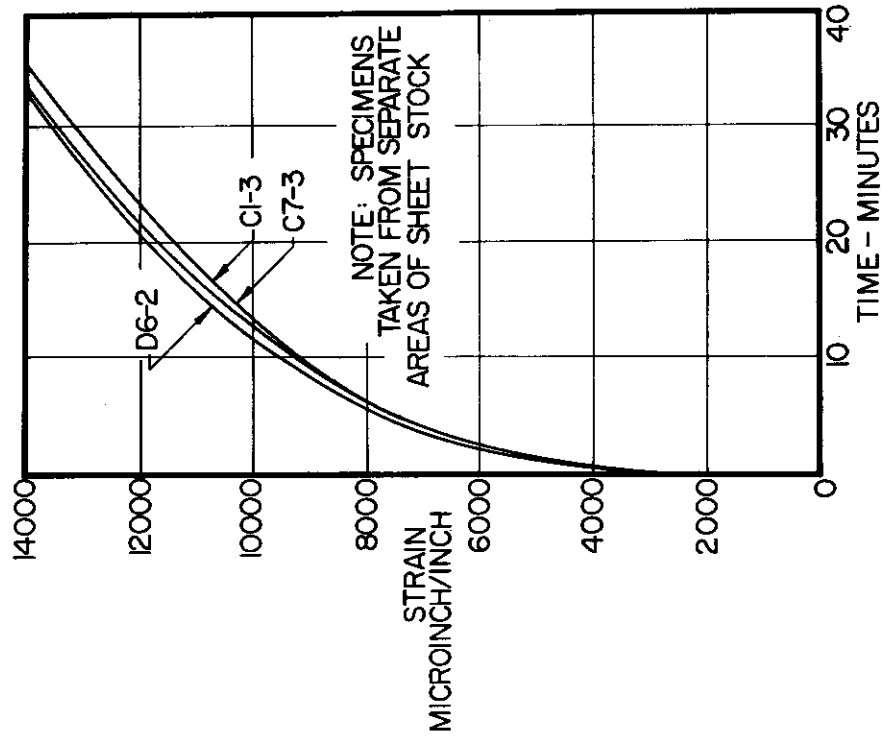


FIGURE 2 PRELIMINARY COMPRESSION CREEP CURVES OF 2024-0 ALUMINUM ALLOY AT 500°F AND 8500 psi APPLIED STRESS USED FOR MATERIAL EVALUATION.

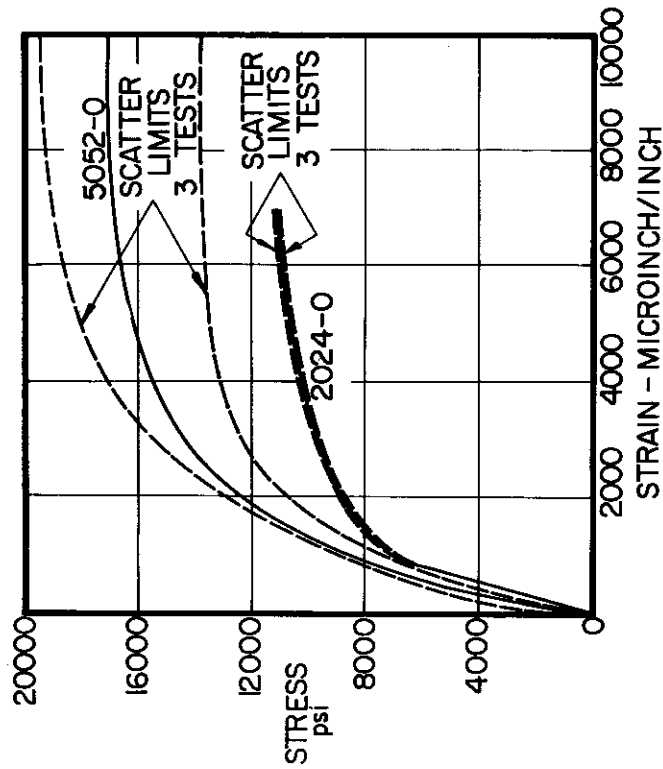


FIGURE 1 COMPARISON OF SHORT TIME STRESS-STRAIN PROPERTIES IN COMPRESSION AT 500°F BETWEEN 2024-0 AND 5052-0 ALUMINUM ALLOY.

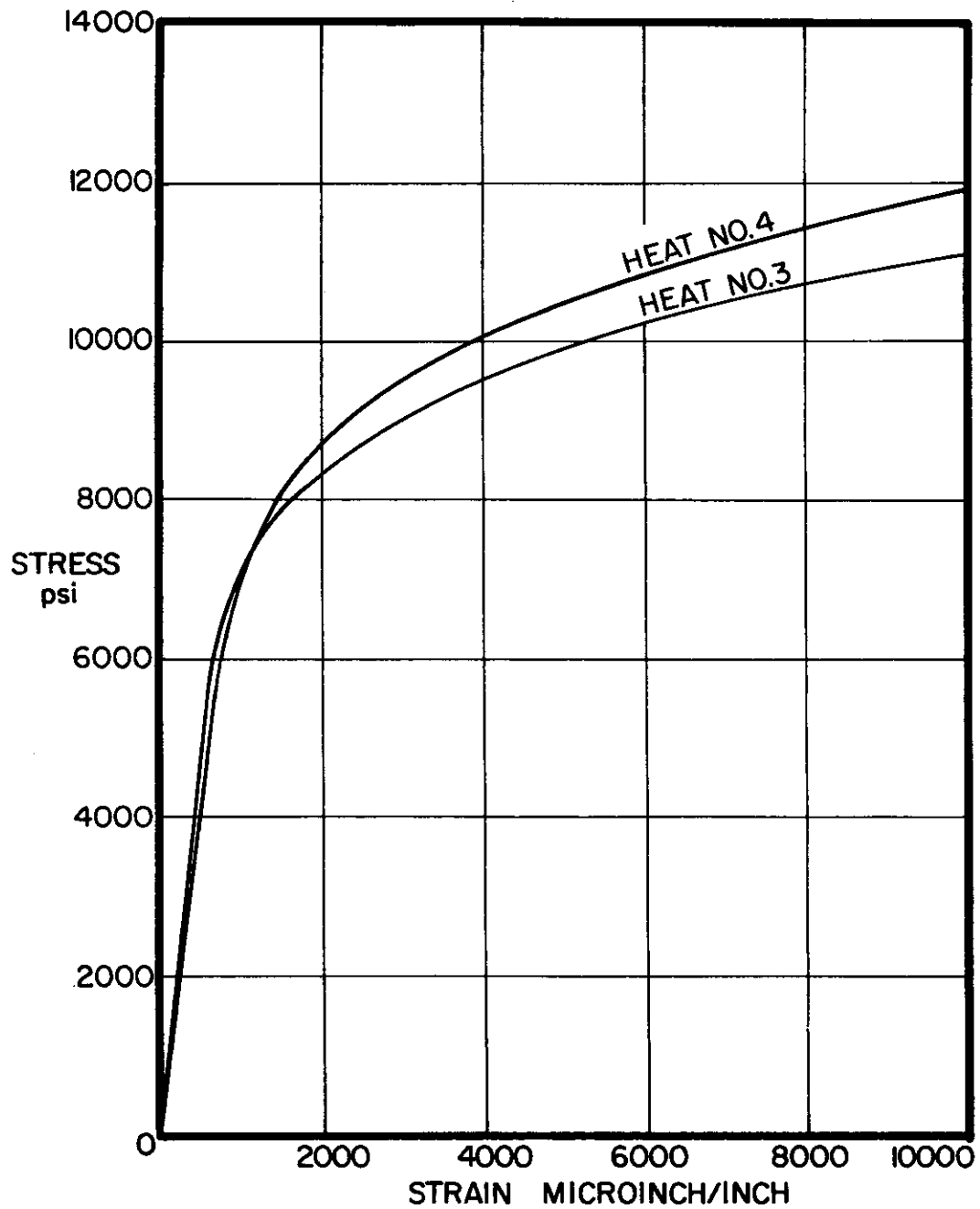


FIGURE 3 AVERAGE SHORT TIME COMPRESSION STRESS-STRAIN CURVES FOR 2024-O ALUMINUM ALLOY AT 500°F.

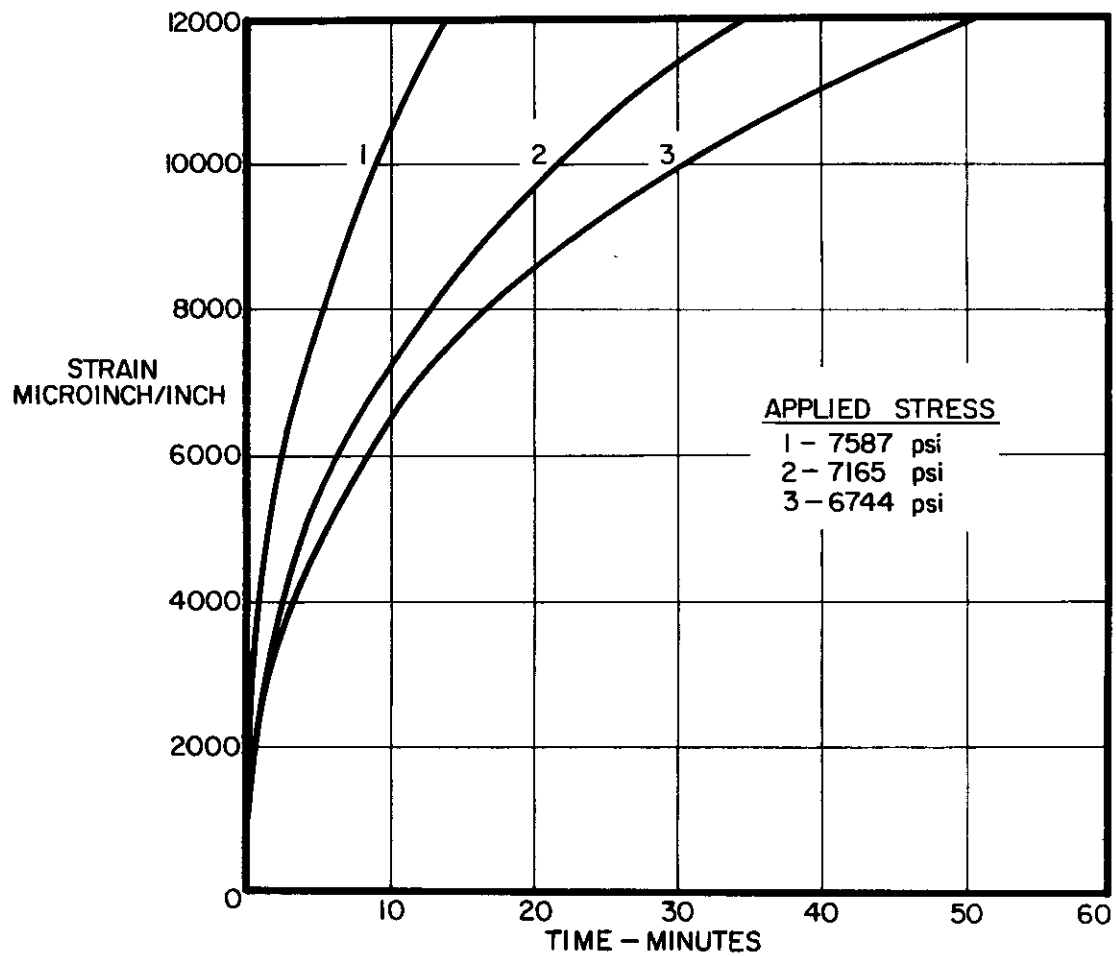


FIGURE 4 AVERAGE COMPRESSION CREEP CURVES FOR 2024-O ALUMINUM ALLOY AT 500°F. HEAT 3.

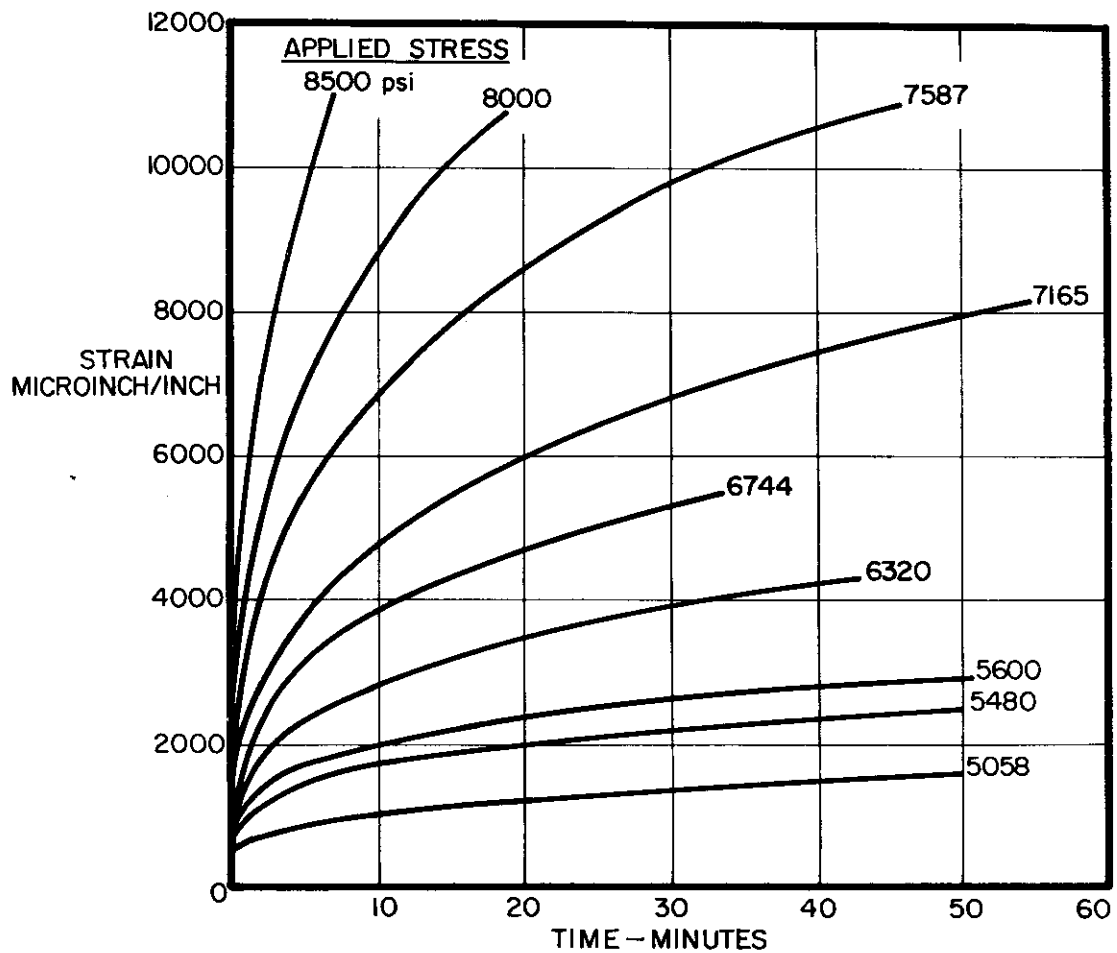


FIGURE 5 AVERAGE COMPRESSION CREEP CURVES FOR 2024-0 ALUMINUM ALLOY AT 500°F. HEAT 4.

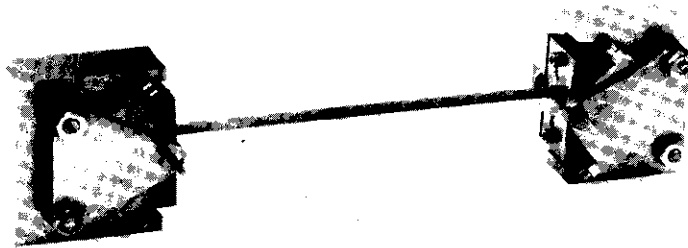


FIGURE 6 ROLLER BEARING END RESTRAINTS SIMULATING SIMPLE SUPPORT.

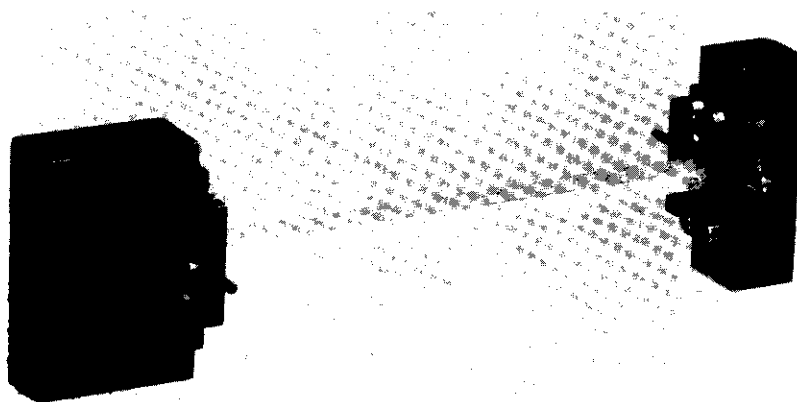


FIGURE 7 FLAT END RESTRAINTS SIMULATING FIXED ENDS.

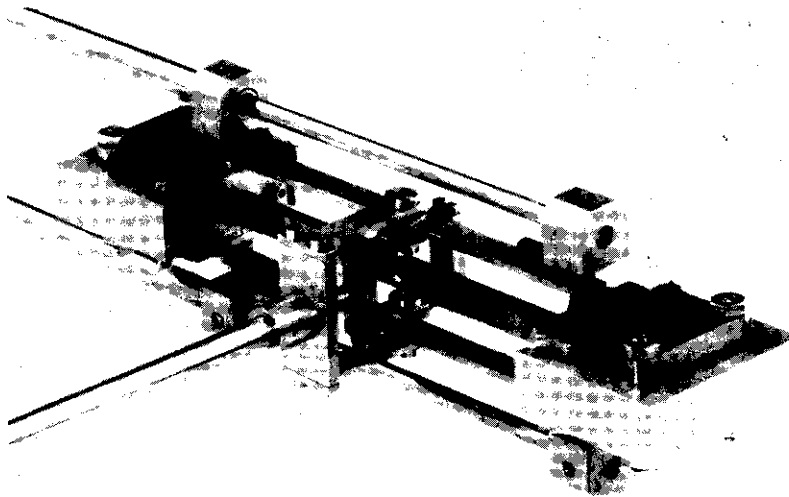


FIGURE 8 COLUMN SPECIMEN INSTALLED IN ROLLER BEARING END RESTRAINTS WITH END SHORTENING AND CENTRAL DEFLECTION INSTRUMENTATION ATTACHED.

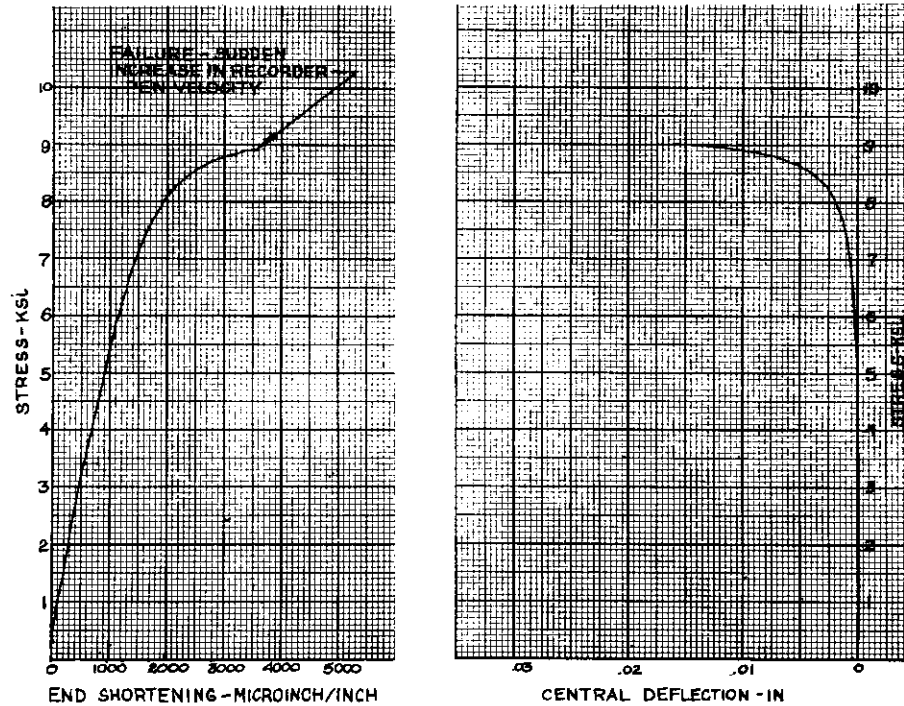


FIGURE 9 TEST RECORDS FOR SHORT TIME BUCKLING TEST OF 2024-O ALUMINUM ALLOY COLUMN, $L'/\rho = 40$ WITH ROLLER END RESTRAINTS AT 500°F .

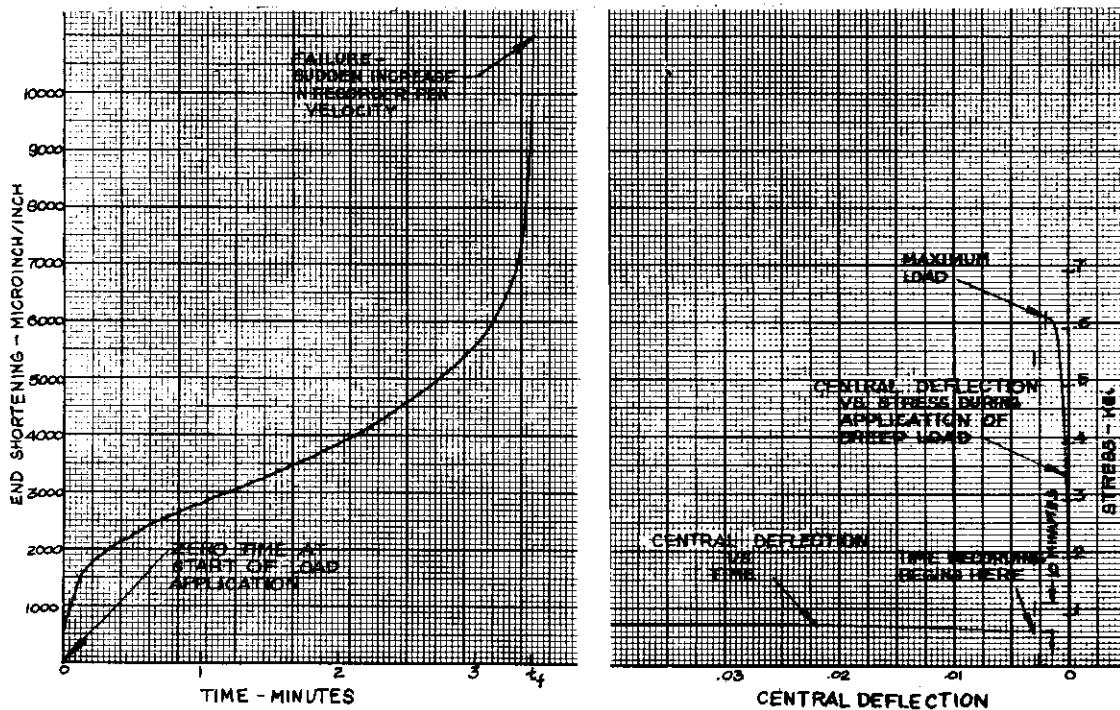


FIGURE 10 TEST RECORDS FOR CREEP BUCKLING TEST OF 2024-O ALUMINUM ALLOY COLUMN, $L'/\rho = 40$ WITH ROLLER END RESTRAINTS AT 6320 PSI AND 500°F .

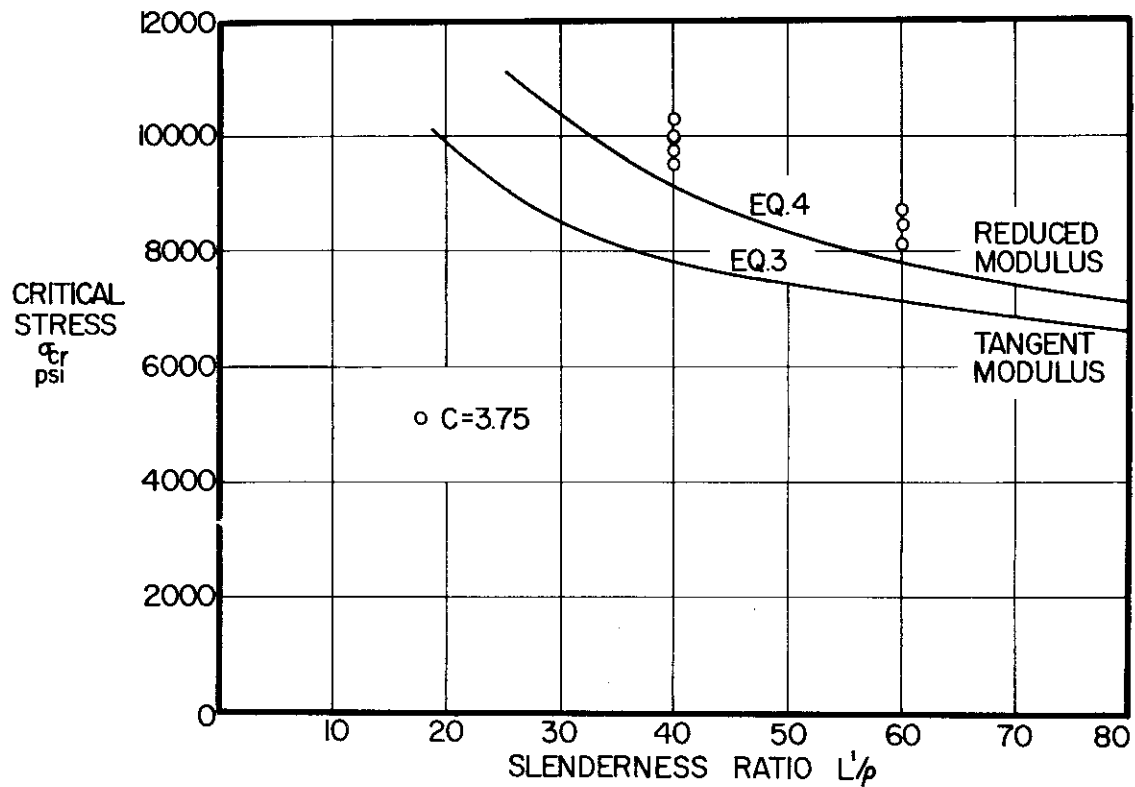


FIGURE 11 SHORT TIME BUCKLING RESULTS FOR ANNEAL HEAT 3 EXPERIMENT AND THEORY.

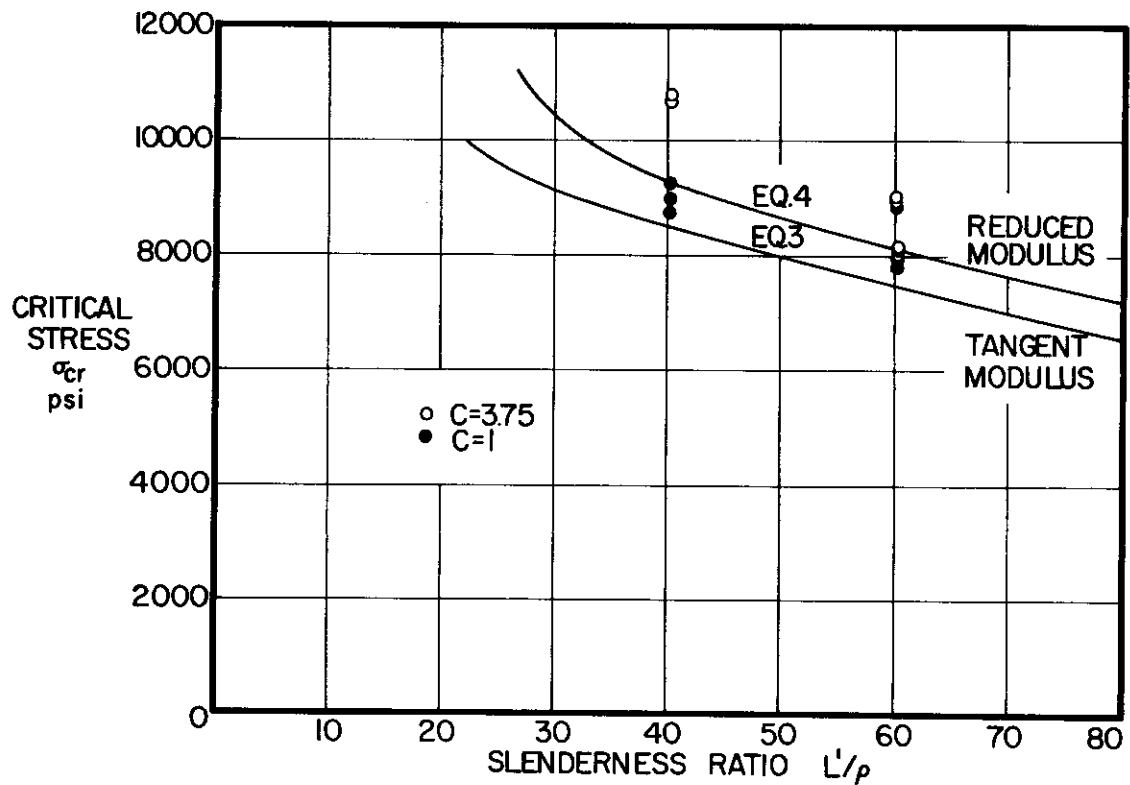


FIGURE 12 SHORT TIME BUCKLING RESULTS FOR ANNEAL HEATS 4 AND 5 EXPERIMENT AND THEORY.

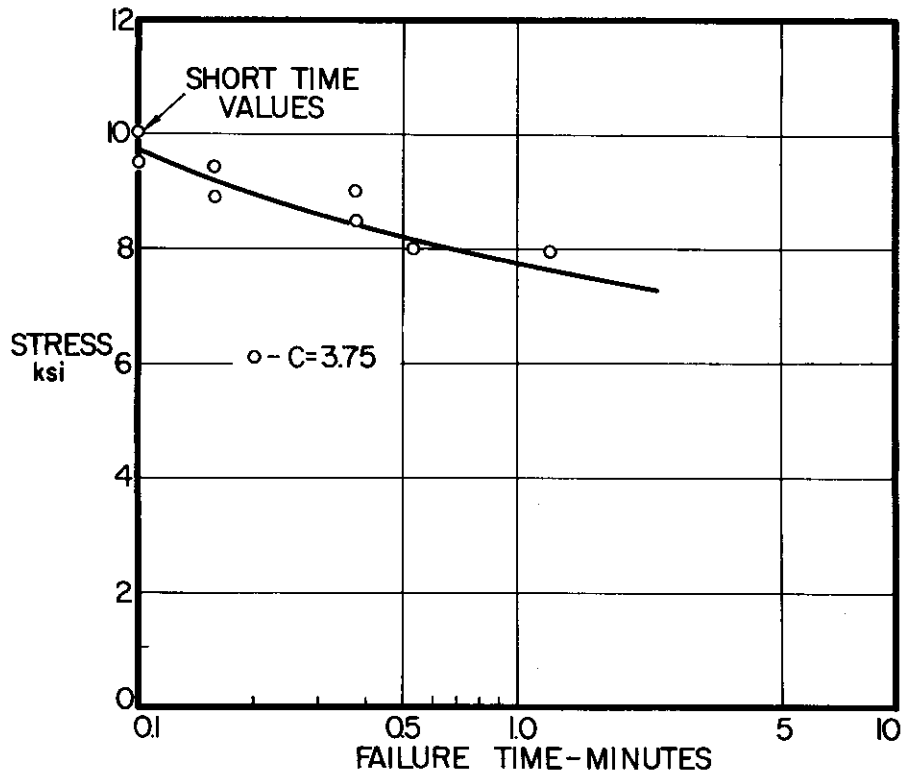


FIGURE 13 CREEP BUCKLING RESULTS FOR COLUMNS OF $L'/\rho = 40$ ANNEAL HEAT 3.

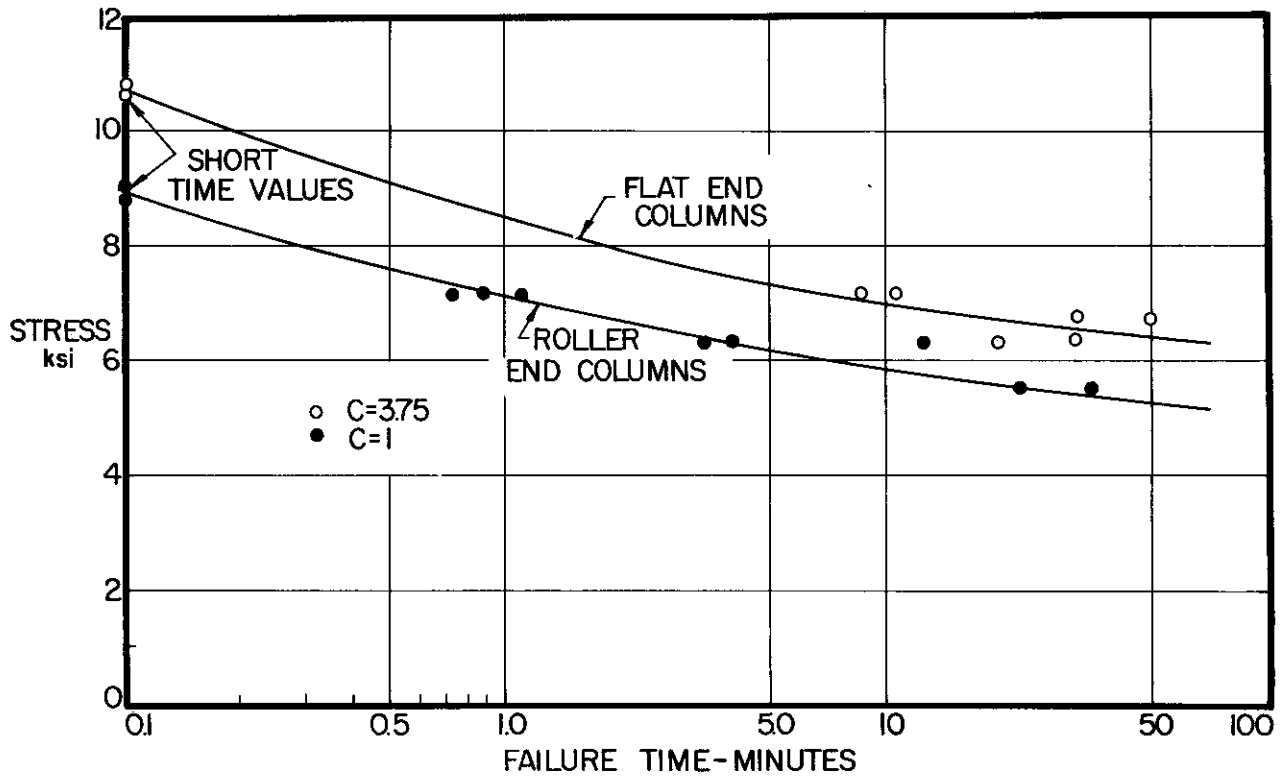


FIGURE 14 CREEP BUCKLING RESULTS FOR COLUMNS OF $L'/\rho = 40$ ANNEAL HEATS 4 AND 5.

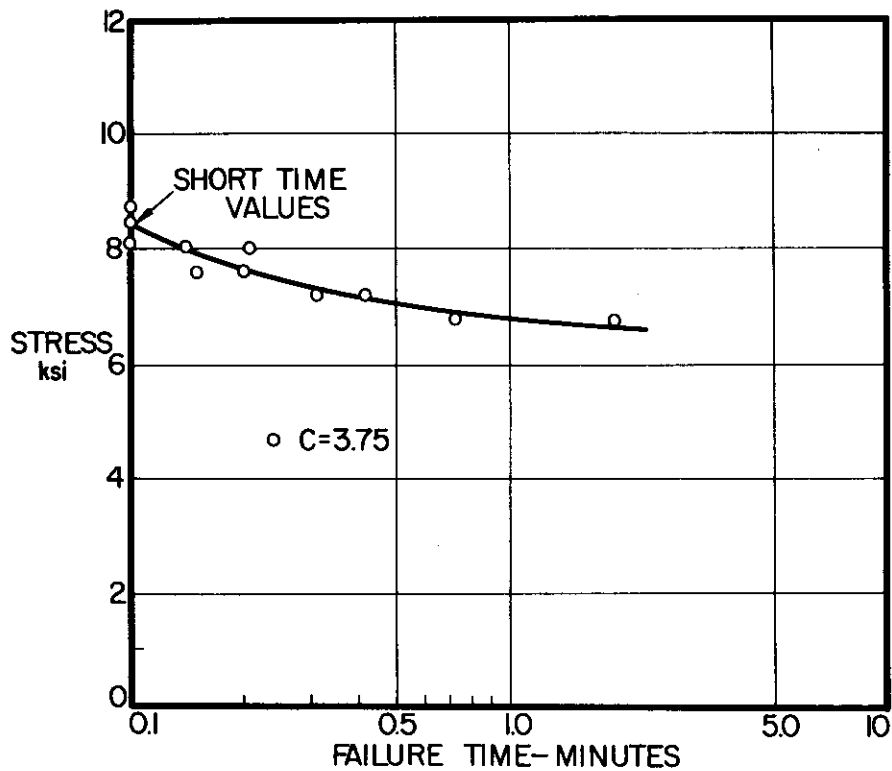


FIGURE 15 CREEP BUCKLING RESULTS FOR COLUMNS OF $L'/\rho = 60$ ANNEAL HEAT 3.

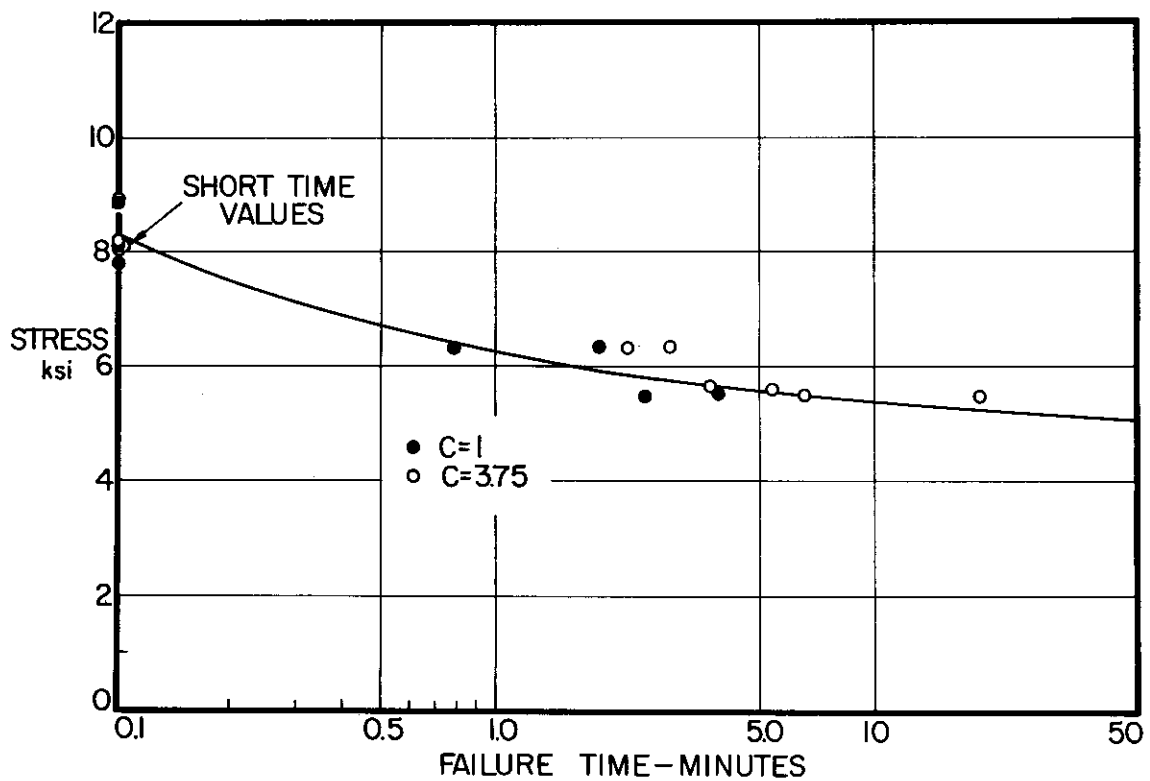


FIGURE 16 CREEP BUCKLING RESULTS FOR COLUMNS OF $L'/\rho = 60$ ANNEAL HEATS 4 AND 5.

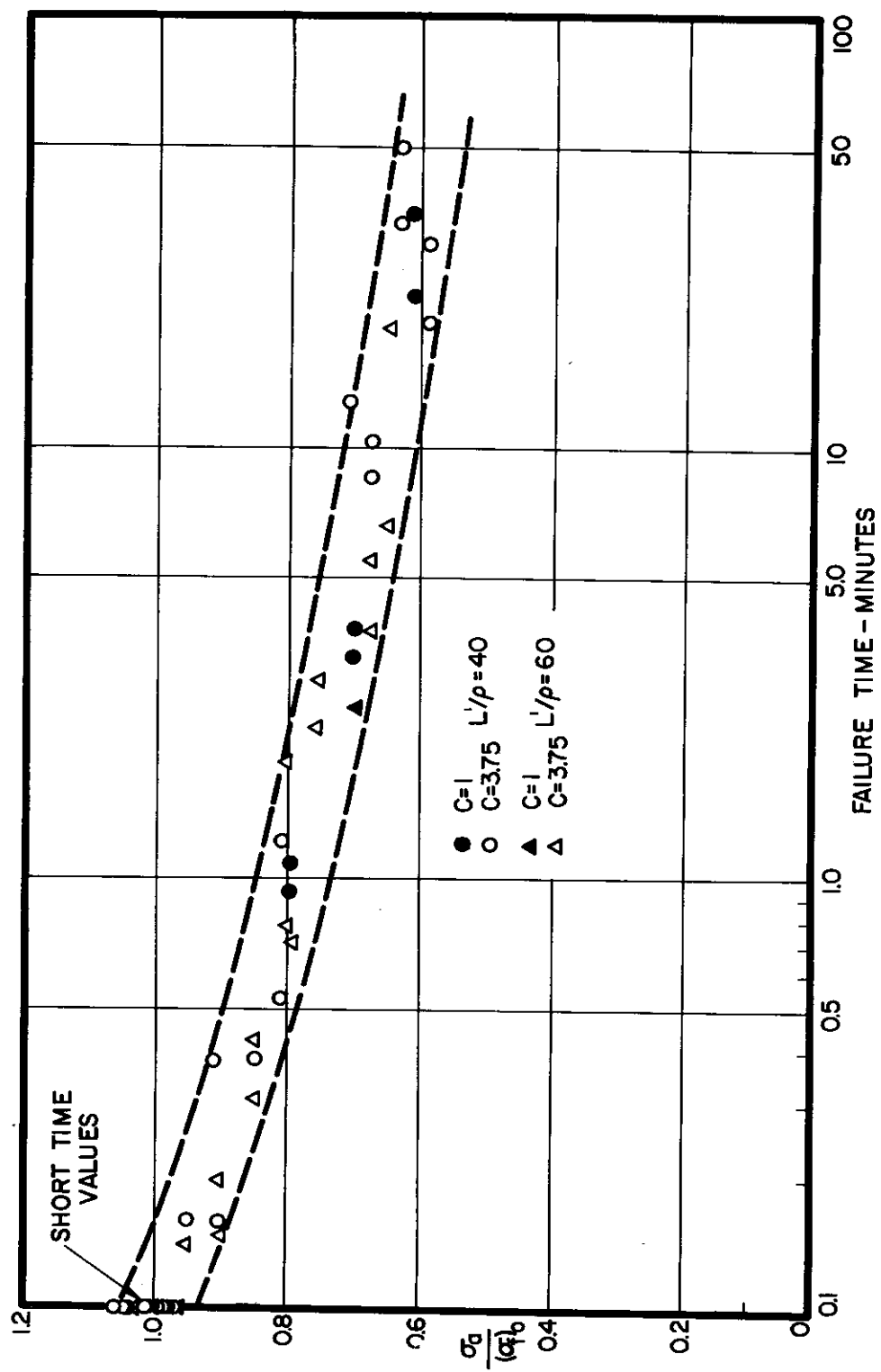


FIGURE 17 NORMALIZED CREEP BUCKLING RESULTS FOR ALL L'/ρ , ALL C VALUES, ALL HEATS.

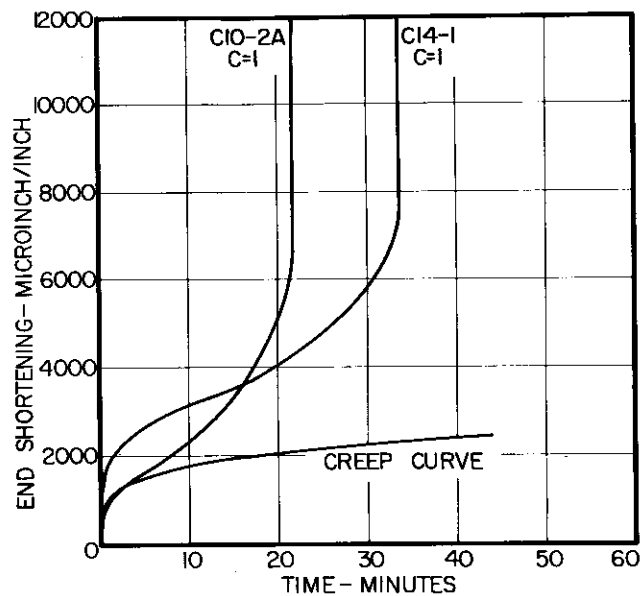


FIGURE 18 END SHORTENING-TIME,
 $L'/\rho = 40$,
 $\sigma_a = 5480$ psi.

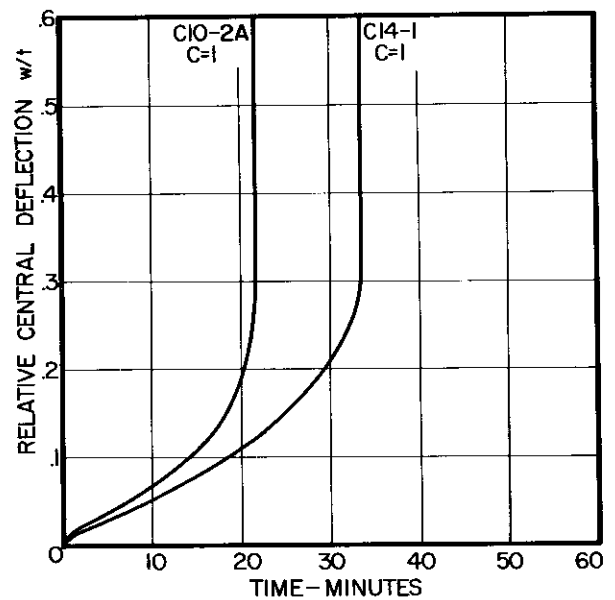


FIGURE 19 CENTRAL DEFLECTION-TIME,
 $L'/\rho = 40$,
 $\sigma_a = 5480$ psi.

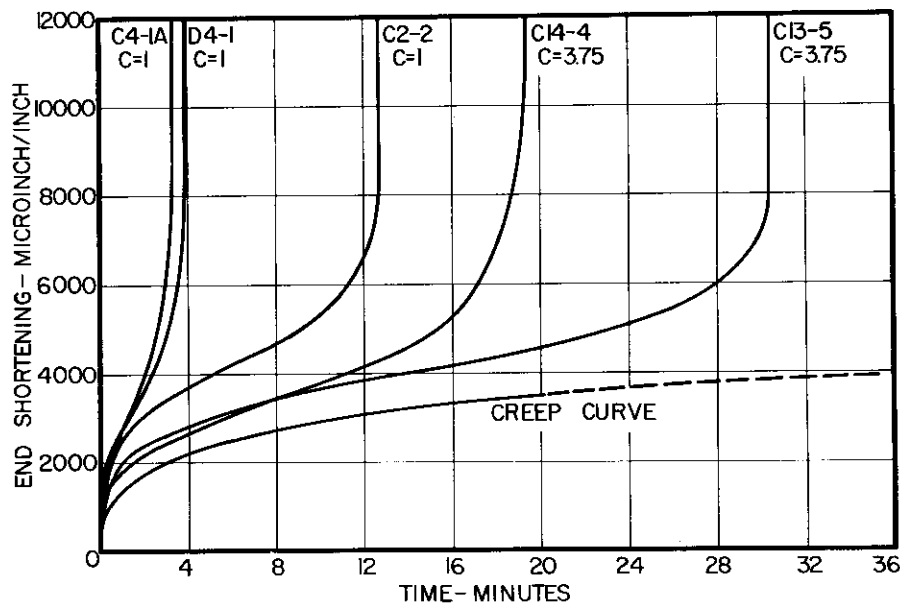


FIGURE 20 END SHORTENING-TIME $L'/\rho = 40$,
 $\sigma_a = 6320$ psi.

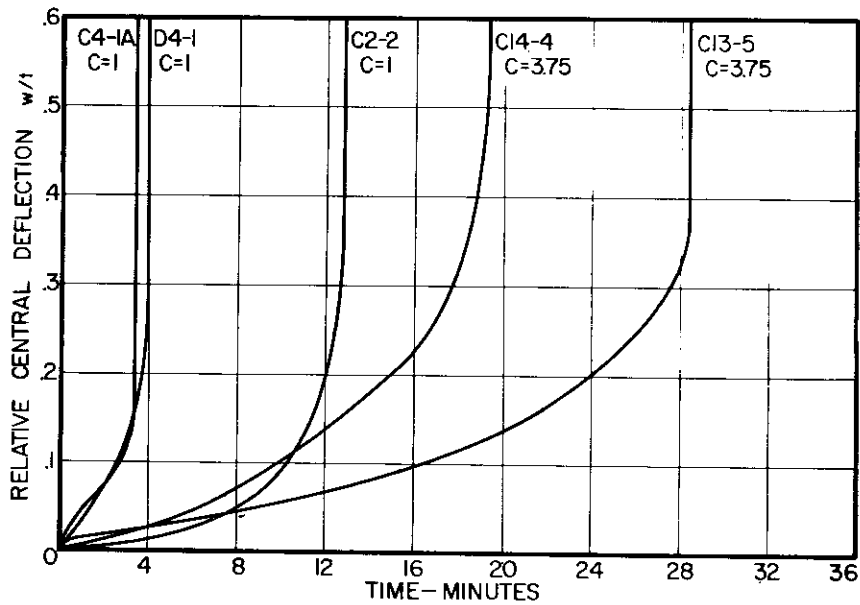


FIGURE 21 CENTRAL DEFLECTION-TIME,
 $L'/\rho = 40$, $\sigma_a = 6320$ psi.

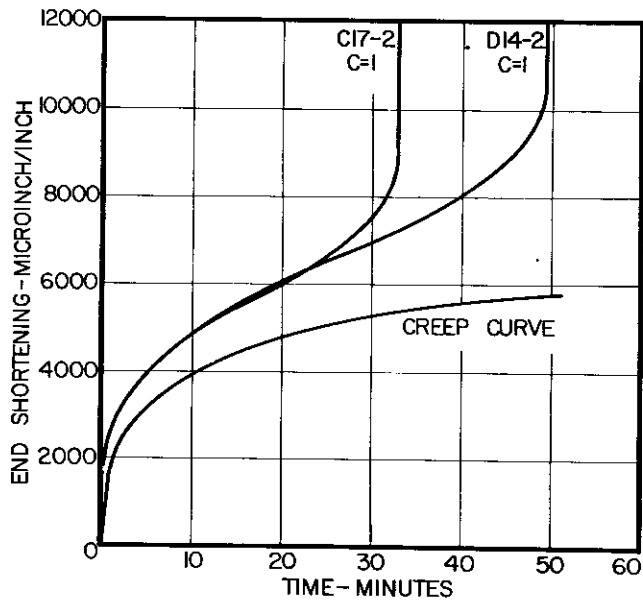


FIGURE 22 END SHORTENING-TIME,
 $L'/\rho = 40$,
 $\sigma_a = 6744$ psi.

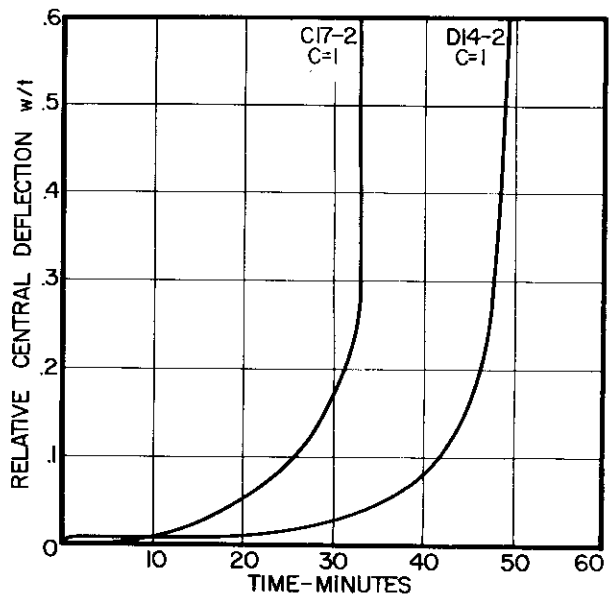


FIGURE 23 CENTRAL DEFLECTION-TIME
 $L'/\rho = 40$,
 $\sigma_a = 6744$ psi.

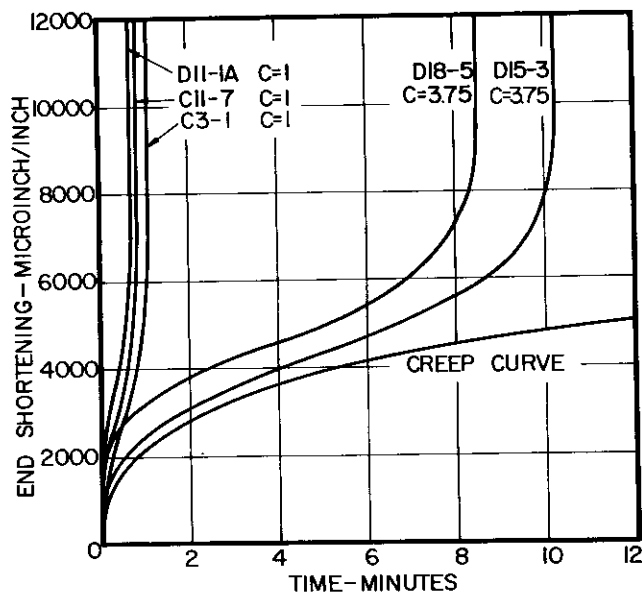


FIGURE 24 END SHORTENING-TIME,
 $L'/\rho = 40$,
 $\sigma_a = 7165$ psi.

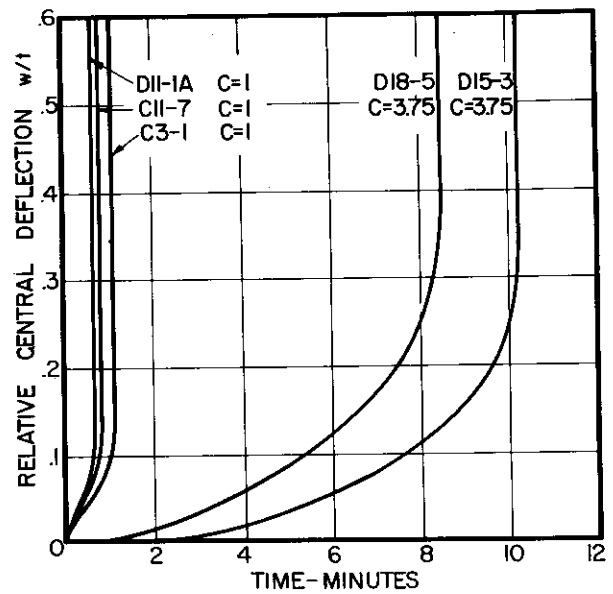


FIGURE 25 CENTRAL DEFLECTION-TIME,
 $L'/\rho = 40$,
 $\sigma_a = 7165$ psi.

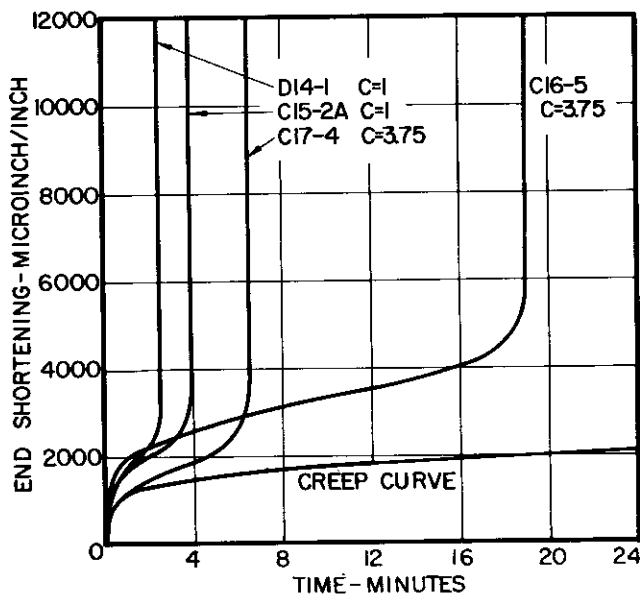


FIGURE 26 END SHORTENING-TIME,
 $L'/\rho = 60$,
 $\sigma_a = 5480$ psi.

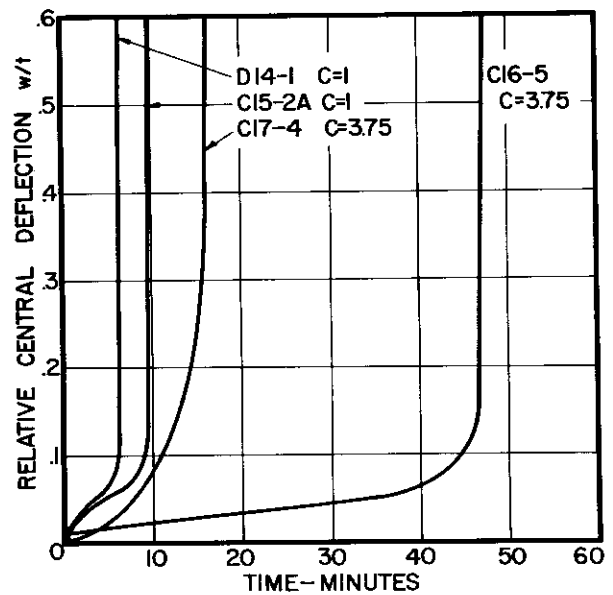


FIGURE 27 CENTRAL DEFLECTION-TIME,
 $L'/\rho = 60$,
 $\sigma_a = 5480$ psi.

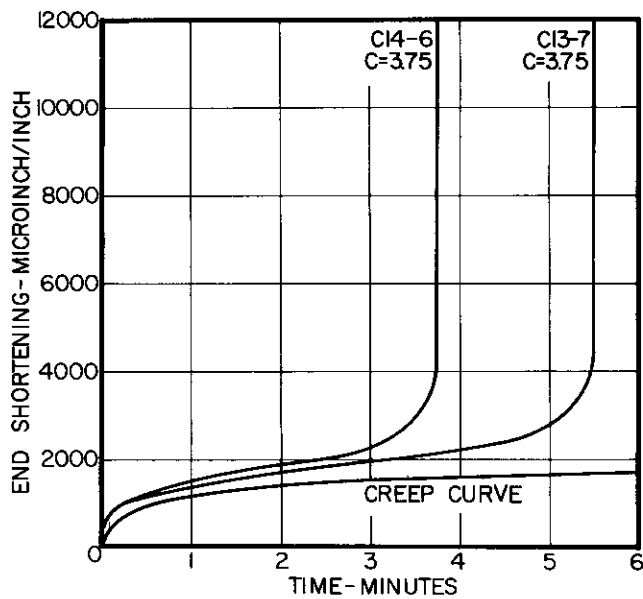


FIGURE 28 END SHORTENING-TIME,
 $L'/\rho = 60$,
 $\sigma_a = 5600$ psi.

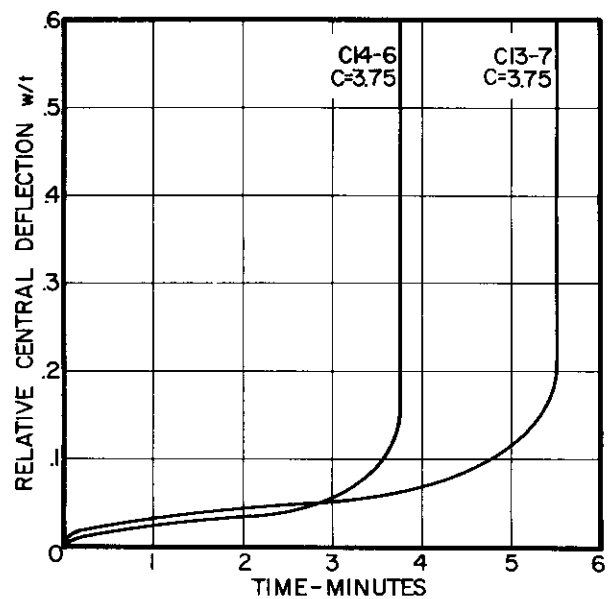


FIGURE 29 CENTRAL DEFLECTION-TIME,
 $L'/\rho = 60$,
 $\sigma_a = 5600$ psi.

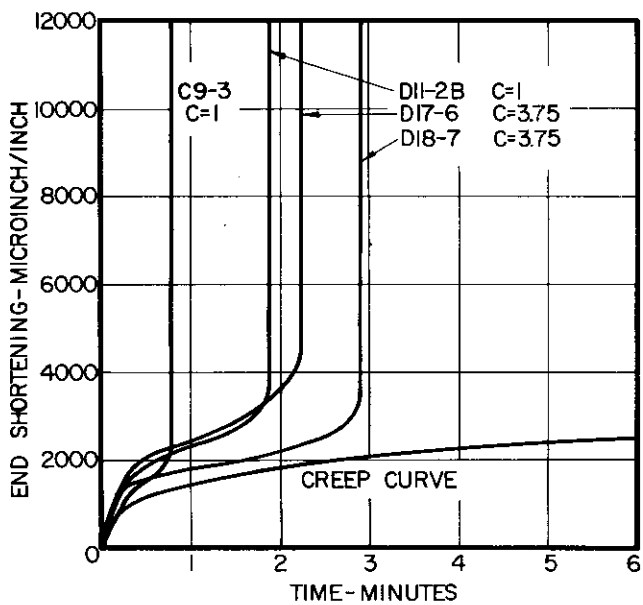


FIGURE 30 END SHORTENING-TIME,
 $L'/\rho = 60$,
 $\sigma_a = 6320$ psi.

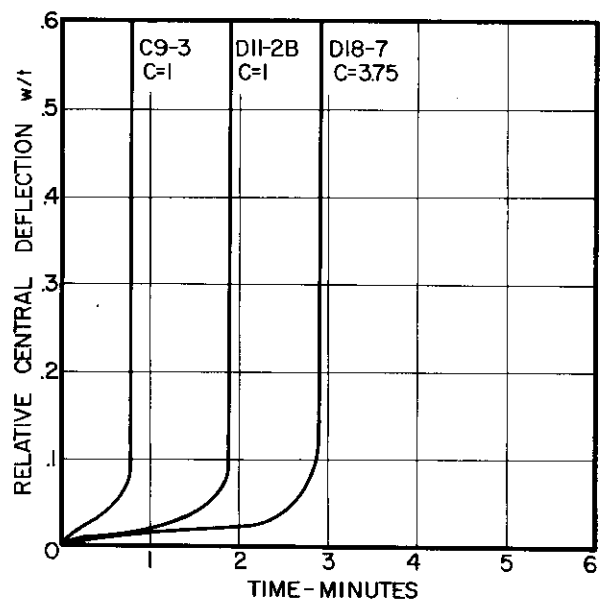


FIGURE 31 CENTRAL DEFLECTION-TIME,
 $L'/\rho = 60$,
 $\sigma_a = 6320$ psi.

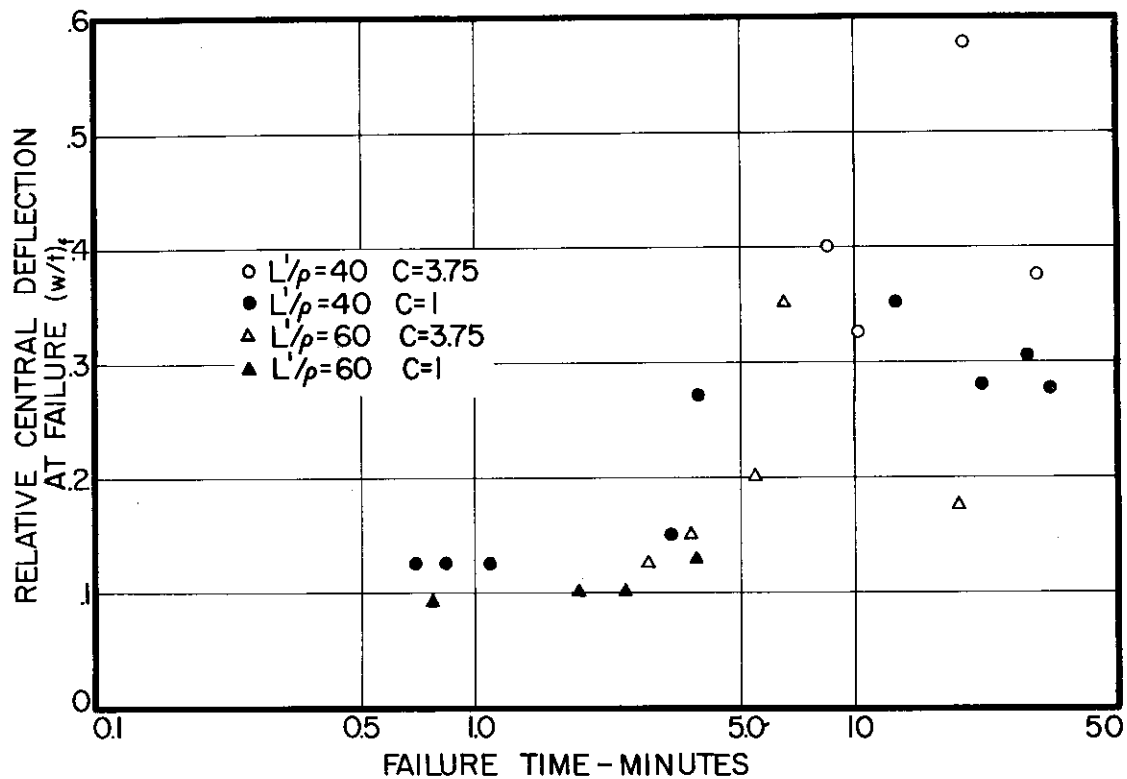


FIGURE 32 RELATIVE CENTRAL DEFLECTION AT FAILURE IN CREEP BUCKLING.

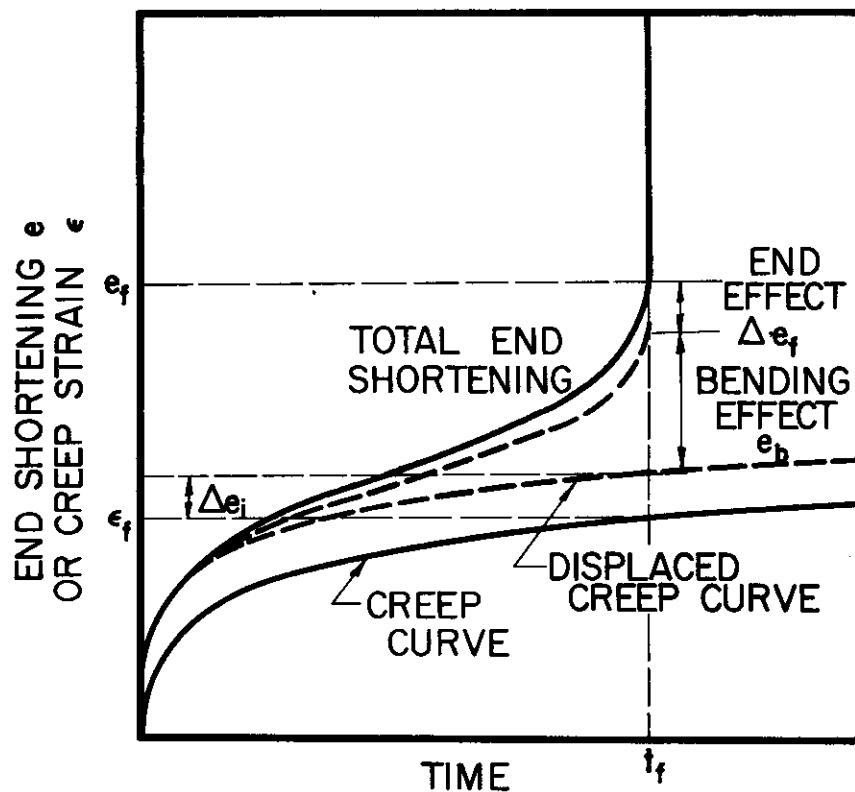


FIGURE 33 DIAGRAM OF TYPICAL END SHORTENING BEHAVIOR.

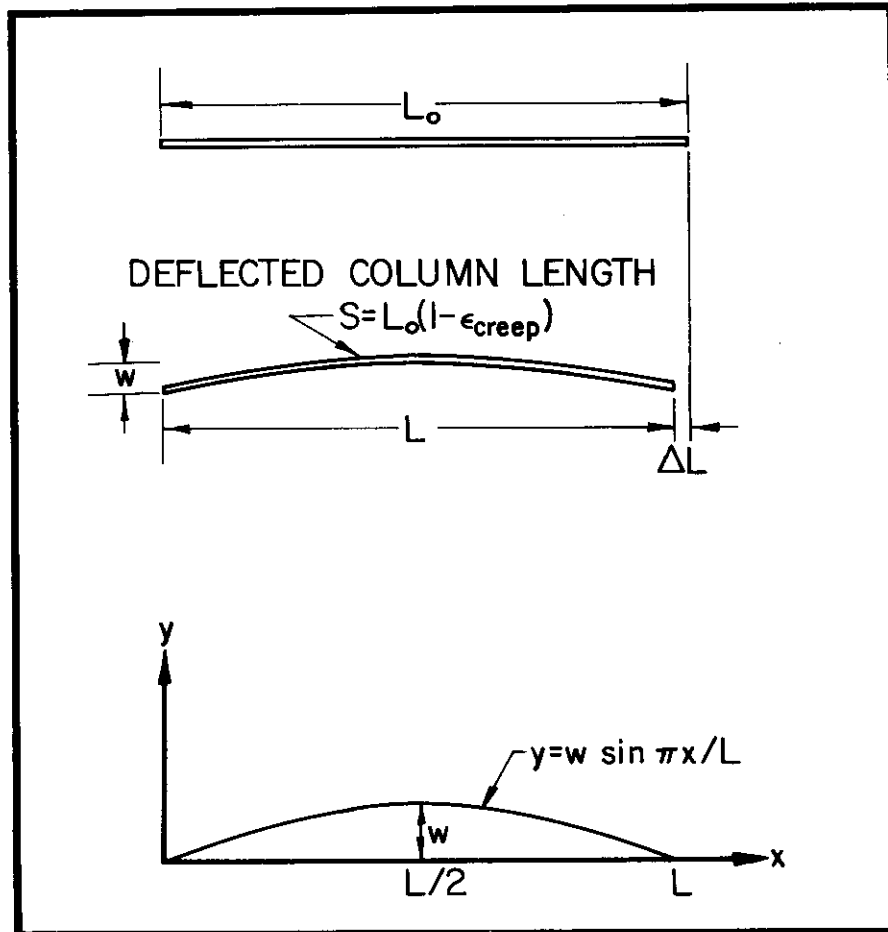


FIGURE 34 DEFLECTED COLUMN GEOMETRY.

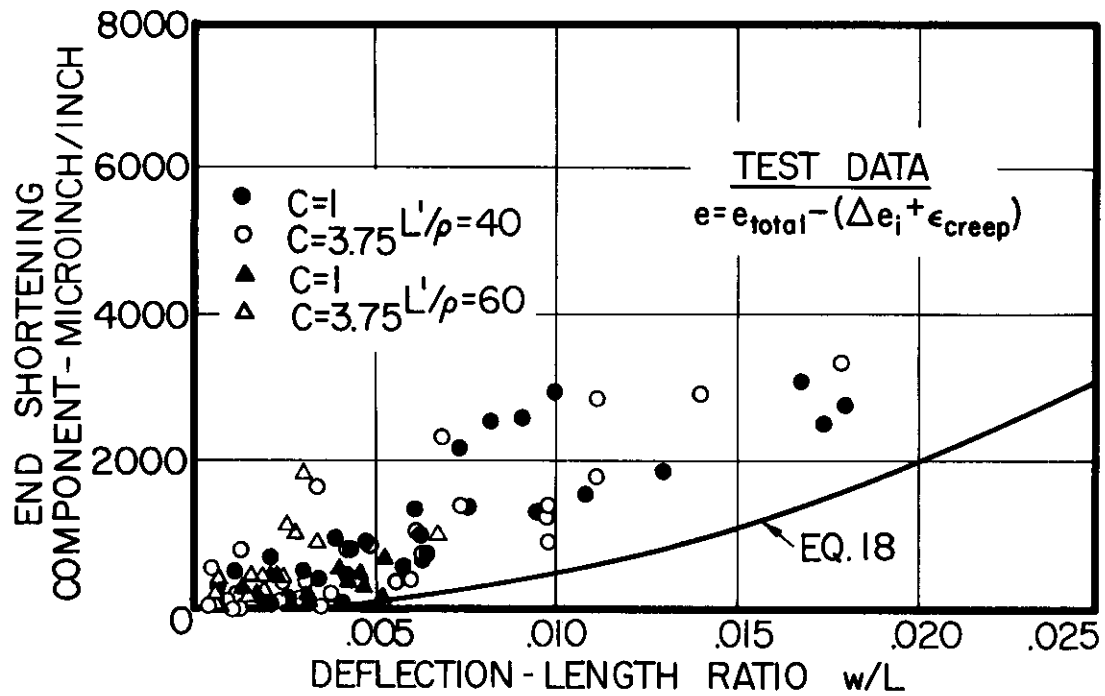


FIGURE 35 THEORETICAL BENDING COMPONENT OF END SHORTENING COMPARED WITH TEST DATA FOR ALL CREEP BUCKLING EXPERIMENTS.

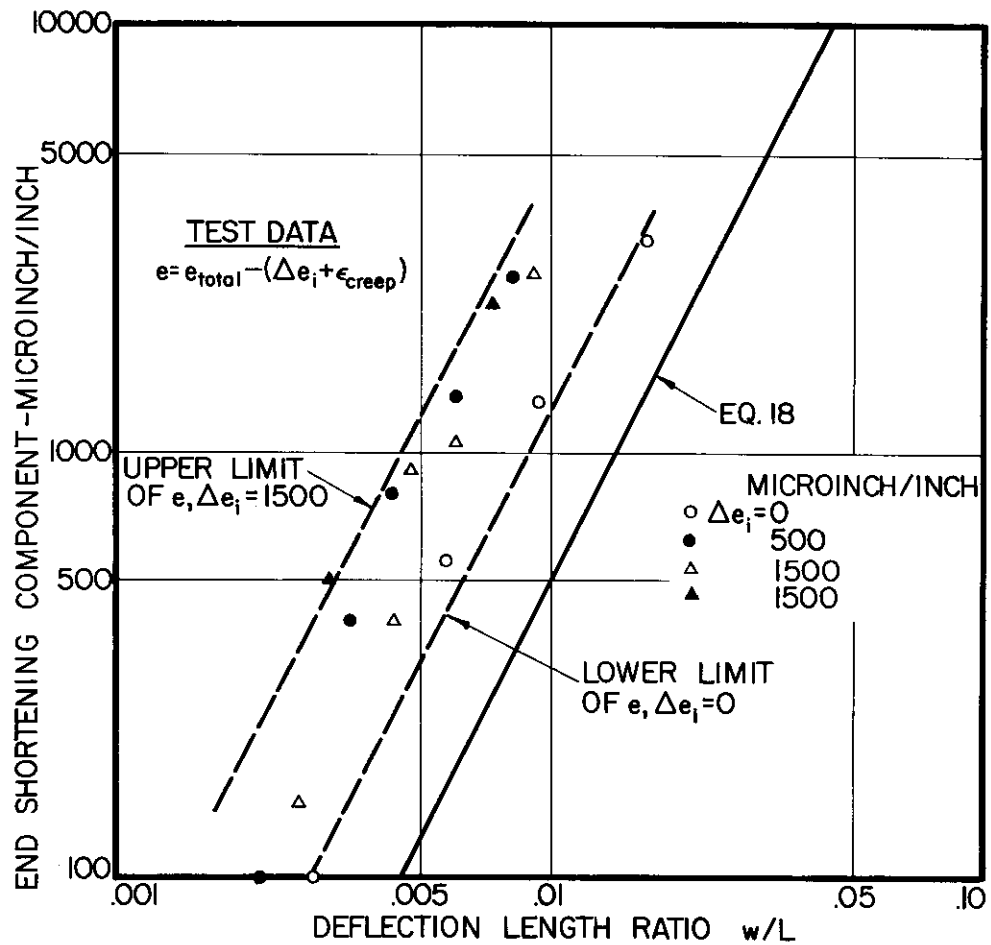


FIGURE 36 THEORETICAL BENDING COMPONENT OF END SHORTENING COMPARED WITH TEST DATA FROM FOUR EXPERIMENTS WITH DIFFERENT INITIAL END SHORTENING COMPONENTS.